Title:

Association of secondary metabolite gene clusters with host-specific lineages of the cereal blast fungus *Pyricularia oryzae*

Khyati Mehta[1,$], Jorge C. Navarro-Muñoz[2,#], Sayali Bakore[3], Jérôme Collemare[2,*] and Rajesh Patkar[1,3,*]

[1] *Bharat Chattoo Genome Research Centre, Department of Microbiology and Biotechnology Centre, The Maharaja Sayajirao University of Baroda, Vadodara, India*

[2] *Westerdijk Fungal Biodiversity Institute, Utrecht, the Netherlands*

[3] *Department of Biosciences & Bioengineering, Indian Institute of Technology Bombay, Mumbai, India*

[$] *Current address: Westerdijk Fungal Biodiversity Institute, Utrecht, the Netherlands*

[#] *Current address: Wageningen University and Research, Wageningen, the Netherlands*

[*] Author for correspondence – Rajesh Patkar - rajeshpatkar@iitb.ac.in and Jérôme Collemare - j.collemare@wi.knaw.nl

Abstract

Fungal plant pathogens constantly evolve and deploy novel peptide and metabolite effectors to break down plant resistance and adapt to new host plants. The blast fungal pathogen *Pyricularia oryzae* is a single species subdivided into multiple host-specific lineages that have evolved through gain and/or loss of virulence and/or effector related genes through chromosomal rearrangement. Here, we mined 68 genomes of *P. oryzae*, belonging to six host-specific lineages, to identify secondary metabolite (SM) biosynthetic gene clusters (BGCs) likely associated with potential metabolite effectors involved in host specialization. A similarity network analysis grouped a total of 4501 BGCs into 283 gene cluster families (GCFs), based on the content and architecture of the BGCs. While most of the GCFs were present in all the *P. oryzae* lineages, two (BGC-O1 and BGC-O2) were found specifically in the *Oryza* lineage and one (BGC-TLE) was found in the lineage specific to *Triticum, Lolium* and *Eleusine* hosts. Further analysis of the phylogenetic relationships between core biosynthetic genes confirmed that BGC-O1, which comprises a reducing polyketide synthase gene (MGG_08236) and four putative tailoring genes, was present only in the *Oryza* lineage. Importantly, most genes, including MGG_08236, from the BGC-O1 were expressed specifically during pathogenesis. We propose that the *Oryza* lineage-specific BGC-O1 produces a metabolite effector likely involved in specialization of *P. oryzae* to the rice host. In addition, we identified five SM genes under positive or balancing selection only in the *Oryza* lineage, suggesting a role in the interaction with rice specifically. Our findings highlight the importance of further mining novel metabolite effectors in specialization and virulence of the blast fungus to different cereal hosts.

Keywords

Biosynthetic diversity, population genomics, *Magnaporthe oryzae,* gene cluster family, polyketide synthase, effector, polymorphism, divergence

48 **Background**

49

50 Many plant pathogenic fungi are adapted to infect specific host plants. The emergence of new
51 pathogenic strains, as a result of host range expansion or specialization to a new host, can
52 cause severe disease outbreaks (Giraud et al., 2010). It is crucial to understand the molecular
53 basis of such host specialization to increase the durability of crop resistance to diseases
54 (Giraud et al., 2010; Gladieux et al., 2014). The filamentous fungus *Pyricularia oryzae*
55 (synonym *Magnaporthe oryzae*) is the causative agent of the economically important cereal
56 blast disease worldwide, and is a model organism to study host-pathogen interactions (Ebbole,
57 2007; Talbot, 2003). Although capable of infecting several grasses, *P. oryzae* is classified as a
58 single species, subdivided into several host-specialized lineages with limited primary host
59 range (Gladieux et al., 2018).

60 Host selection pressure could be one of the factors that shape the virulence of the population
61 of a pathogen, whereby specific virulence-related genes that encode secreted proteins and/or
62 enzymes for secondary metabolite production - collectively known as effectors – are either
63 gained or lost (Hartmann et al., 2018; Zhong et al., 2016). Effectors manipulate the host
64 physiology or immunity to the pathogen's advantage, and thus are major determinants of
65 specialization on a host (Sánchez-Vallet et al., 2018). Indeed, gain- or loss-of-function
66 mutation in avirulence (AVR) genes of *P. oryzae* has resulted in overcoming host resistance
67 or non-host resistance in case of a new host. For example, a widespread cultivation of wheat
68 cultivar IAC-5 carrying the *RWT3* resistance gene led to a loss of function of the
69 corresponding *PWT3* AVR gene in *P. oryzae* and subsequent emergence of wheat blast (Inoue
70 et al., 2017). Similarly, although gain of the AVR gene *PWL1* led to a loss of pathogenesis on

71 weeping lovegrass in the *Eleusine*-lineage of *P. oryzae*, it conferred virulence on the new
72 host, finger millet (Asuke et al., 2020). Further, *AVR-Pita*, flanked by retrotransposons, has
73 been found to be translocated to multiple genomic locations, including supernumerary
74 chromosomes, as a result of dynamic adaptation towards its corresponding resistance gene
75 *Pita* in certain rice varieties (Chuma et al., 2011).

76 Fungal secondary metabolites (SMs) have also been shown to exhibit important effector
77 functions during plant-fungal interactions (Collemare et al., 2019). For example, ACE1, a
78 secondary metabolite (SM) produced by *P. oryzae*, confers avirulence towards the rice
79 cultivars carrying the corresponding resistance gene *Pi33* (Böhnert et al., 2004). Various
80 fungal pathogens, including *P. oryzae*, are also known to produce analogues of plant
81 hormones such as jasmonic acid, gibberellin and cytokinins, to manipulate plant growth or
82 subvert plant hormone-based defense signalling pathways during invasion (Patkar & Naqvi,
83 2017; Shen et al., 2018). A derivative of jasmonic acid (12-hydroxyjasmonic acid) secreted by
84 *P. oryzae* suppresses the host innate immunity specifically in rice but not in barley or wheat
85 (Patkar et al., 2015). Many other fungal SMs such as host-selective toxins (HST) also act as
86 virulence factors – for example, HC-toxin in *Cochliobous carbonum*, T-toxin in *C.*
87 *heterostrophus*, AM-toxin and ACR-toxin in *Alternaria alternata* (Izumi et al., 2012; Lim &
88 Hooker, 1971; Tsuge et al., 2013; Walton, 2006). These HSTs are essential for pathogenesis
89 on specific hosts carrying the corresponding susceptible gene. The blast fungus produces SMs
90 such as tenuazonic acid and pyriculol during pathogenesis (Chen & Qiang, 2017; Jacob et al.,
91 2017).

92 The availability of an increasing number of fungal genomes and advances in computational
93 biology facilitates the exploration of molecular determinants of host specialization or host

range expansion. For instance, population genomics of the wheat fungal pathogen *Zymoseptoria tritici* has revealed a possible role of SMs in pathogen lineage diversification and adaptation to wheat host (Hartmann et al., 2018). In *P. oryzae* isolates, specialization to rice host is likely associated with a small number of lineage-specific gene families, which could include genes involved in biosynthesis of SMs and secreted proteins of unknown functions (Chiapello et al., 2015). While most studies have focused on the effector function of certain secreted proteins in the blast fungus, the link between diverse SM biosynthetic gene clusters (BGCs) and *P. oryzae* host-specific lineages has not been explored.

Here, we embarked on the exploration of genomes from the different lineages of the blast fungus, in search for SM BGCs associated with host specialization. Using similarity network, comparative genomics and phylogenetic analyses, we identified a candidate BGC that is likely involved in pathogenesis and specialization to rice and weeping lovegrass host plants.

107 **Results**

108

109 **Genome sequencing of host-specific strains of *P. oryzae***

110 In this study, we used 68 *P. oryzae* genomes isolated from 6 different host plants, rice (*Oryza*
111 *sativa*, n = 26), finger millet *(Eleusine sp.*, n = 14), foxtail millet *(Setaria sp.*, n = 7), wheat
112 (*Triticum aestivum*, n = 12), perennial ryegrass *(Lolium sp.*, n = 8) and weeping lovegrass
113 (*Eragrostis curvula*, n = 1) (Fig. 1A, Supplementary Table S1). These genomes included 15
114 field isolates that were collected from infected rice, finger millet and foxtail millet plants
115 grown in different parts of India (Fig. 1A, Supplementary Table S1) and sequenced using
116 Illumina technology (Supplementary Table S2). The remaining 53 genomes were obtained
117 from publicly available genome sequences (Supplementary Table S1, Fig. 1A). Additionally,
118 sequence data from three *P. grisea* strains previously isolated from crabgrass (*Digitaria sp.)*
119 was used as an outgroup (Supplementary Table S1). Sixteen publicly available assemblies
120 were obtained from long-read sequencing technology and were highly-contiguous. We
121 performed new gene prediction for all 71 assemblies and analysis of BUSCO genes indicated
122 high-quality gene prediction and completeness of the assemblies (with minimum 91.5%,
123 maximum 98.6% and average 96.6% BUSCO-score; Supplementary Table S1).
124 We used 2655 BUSCO genes present in the 68 *P. oryzae* genomes to build a phylogenomic
125 tree (Supplementary dataset S4). The topology of the obtained species tree confirms that *P.*
126 *oryzae* consists of multiple genetic lineages specialized on different hosts, including *Oryza,*
127 *Setaria, Eleusine, Eragrostis, Triticum* and *Lolium* (Fig. 1B). This tree is concordant with the
128 previously reported population structure (Gladieux et al., 2018). A similar phylogenomic
129 analysis, using additional three genomes from *P. grisea* (*Digitaria* isolates), showed that *P.*

130 *grisea* is a separate species from *P. oryzae*, which is consistent with a previously reported
131 study (Supplementary Fig. S1; Supplementary dataset S7; Gladieux et al., 2018).
132 We performed infection assays to check the pathogenesis of 16 Indian isolates of *P. oryzae* on
133 three hosts – rice, finger millet and foxtail millet. We found that all isolates but one (*P. oryzae*
134 MOS1 strain) induced clear blast lesions on their host-of-origin, while they triggered no or
135 few symptoms on non-hosts (Supplementary Fig. S2). In several cases, small dark necrotic
136 spots were observed, indicative of a hypersensitive response caused by recognition of the
137 strain (Supplementary Fig. S2). Intriguingly, MOS1 and MOS4, two strains isolated from
138 infected rice leaf tissue, were found to be genetically similar to that of the *Eleusine* lineage
139 and not related to any lineage, respectively (Fig. 1B). The whole-plant infection assay using
140 the MOS1 strain showed differential virulence pattern, where inoculated finger millet and rice
141 plants developed highly-susceptible and moderately-resistant lesions, respectively, similar to
142 other isolates from finger millet (Supplementary Fig. S2). This result indicates that MOS1 is
143 indeed an *Eleusine* lineage strain which was isolated from infected rice tissue. It is possible
144 that the strain MOS1 could be evolving to adapt to rice host, or it randomly landed on the
145 collected rice leaf and benefited from a co-infection by an *Oryza* lineage strain. Further
146 studies are required to understand whether it was associated with any co-infection of the
147 concerned rice plant tissue with two genetically distinct *P. oryzae* strains. Further, although
148 genetically not similar to any specific lineage, the MOS4 strain showed similar virulence
149 pattern – a few susceptible lesions and small necrotic spots - as that by the *Oryza* lineage
150 strains MOS3 and MOS5 (Supplementary Fig. S2). These results suggest that MOS4 strain
151 defines a separate lineage that can infect rice, yet it may have another primary host that
152 remains to be determined.

153

154 **Genome mining identified lineage-specific biosynthetic gene clusters in *P. oryzae***

155 The identification of genomic regions that contain SM BGCs was performed in all 71
156 genomes using antiSMASH (Blin et al., 2021). This analysis resulted in predicting a total of
157 4224 BGCs, with an average number of 59 BGCs per strain (Supplementary Table S3). The
158 predicted BGCs were classified based on the core biosynthetic genes, such as genes encoding
159 polyketide synthases (PKSs), non-ribosomal peptide synthetases (NRPSs) or terpene cyclases
160 (TCs) (Supplementary Fig. S3, Supplementary Table S3). All the host-specific lineages
161 contained similar number of BGCs from all different classes of BGCs, with type I PKSs being
162 the most abundant (Supplementary Fig. S3). Overall, these analyses highlight the great
163 potential of *P. oryzae* in producing a diverse set of SMs, some of which could be involved in
164 virulence and/or host specialization.

165 In order to understand the role of SM genes during divergence of the *Oryza* lineages, we
166 assessed natural selection by determining the polymorphism within populations and
167 divergence between the *Oryza*, *Triticum* and *Eleusine* populations in SM core biosynthetic
168 genes shared by at least ten isolates from each host-specific lineage. We found that most SM
169 core biosynthetic genes are either under strong or relaxed purifying selection in all three
170 lineages (Supplementary Table S4). For instance, core genes in the melanin and ACE1
171 biosynthetic pathways are under strong purifying selection, which is consistent with their key
172 roles in the interaction of the fungus on any host species (Chumley & Valent, 1990; Fudal et
173 al., 2007; Vy et al., 2024). Only four SM core enzyme genes (MGG_00806, MGG_01951,
174 MGG_03401 and MGG_04775) were found to be under balancing selection in the *Oryza*
175 lineage, and two of these genes were found to be upregulated in appressoria during host
176 penetration (Oh et al., 2008; unpublished data). Interestingly, one gene MGG_09239 is under

177 positive selection in the *Oryza* lineage only (Supplementary Table S4). These observations
178 suggest that only a handful of SM genes likely have a role during interaction with rice
179 specifically. Especially, genes under balancing selection could be involved in the arms race
180 with the rice host and represent interesting targets for future functional studies (Brunner &
181 McDonald, 2018; Oliva et al., 2015; Van Der Hoorn, 2002).
182 To determine if any putative BGC is associated with the ability to infect specific host plants,
183 we performed a network similarity analysis using BiG-SCAPE (Navarro-Muñoz et al., 2019).
184 This analysis included the 4224 predicted BGCs and 277 characterized BGCs from the
185 MIBiG database (Kautsar et al., 2019) used as a reference. The 4501 BGCs were clustered
186 into 283 gene cluster families (GCFs)/subnetworks, of which 180 are singletons, including
187 160 from the reference characterized BGCs (Fig. 2). Twelve out of 91 GCFs present in
188 *Pyricularia* strains comprised a characterized BGC, including largely conserved ones for
189 DHN melanin, epipyriculol, alternapyrone, squalestatin and cytochalasins in *P. oryzae*, and
190 betaneone in *P. grisea* (Fig. 2; Supplementary Fig. S4-S8). Forty-four GCFs are found in
191 several *P. oryzae* lineages as well as in *P. grisea*, most of which remain uncharacterized.
192 Interestingly, 13 and 14 out of 91 GCFs appeared to be specific to *P. grisea* and *P. oryzae*,
193 respectively (Fig. 2). Of the *P. oryzae*-specific GCFs, three were potentially associated with
194 host specific lineages. While BGC-O1 and BGC-O2 were found mostly specific to the *Oryza*
195 lineage, BGC-TLE was found specific to *Tritici*, *Lolium, Eleusine* and *Eragrostis* lineages
196 (Fig. 2), which all share a common origin and diverged from the *Oryza* and *Setaria* lineages
197 (Fig. 1). BGC-O1 consists of genes encoding a reducing PKS and tailoring enzymes (see
198 below), whereas BGC-O2 is restricted to a truncated PKS gene alone that is likely not
199 functional (Supplementary Fig. S9). In the case of BGC-TLE, although the standalone core
200 biosynthetic NRPS gene therein is present in all the strains, the gene structure appeared

201 different (Supplementary Fig. S10). Manual curation of the NRPS gene showed the deletion
202 of 557 bp in *Triticum* and *Lolium* lineages corresponding to the second exon in the *Eleusine*
203 lineage (CD156 strain). Further, the presence of a stop codon within the adenylation domain
204 of the NRPS gene in the *Triticum* and *Lolium* lineages suggests pseudogenization. BGC-TLE
205 is thus likely not functional in those strains (Supplementary Fig. S11). Yet, it could be either
206 important for virulence on *Eleusine* host plants only, or its product might have an avirulence
207 effector-like role in *Triticum* and *Lolium* hosts. Thus, out of three candidate BGCs, we further
208 investigated BGC-O1 as potentially involved in specialization on rice and weeping lovegrass
209 hosts.
210
211 **A novel polyketide biosynthetic gene cluster specifically found in rice/Eragrostis-**
212 **infecting lineage of *P. oryzae***
213 BGC-O1 was found in 23 out of the 24 *Oryza* lineage strains used in the study, as well as in
214 one *Eragrostis* lineage strain (Fig. 3). This GCF appeared to contain two different networks,
215 and comparison of the loci indeed clearly differentiated two putative BGCs - one conserved in
216 all lineages, and BGC-O1 restricted to the *Oryza* and *Eragrostis* lineages (Fig. 3). BGC-O1
217 contains a novel reducing PKS gene (MGG_08236) as the core biosynthetic gene along with
218 flanking tailoring genes, including one methyl transferase (MGG_15107), two cytochrome
219 P450 monooxygenases (MGG_12496 and MGG_12497) and one Co-A transferase
220 (MGG_15108).
221 To assess if only the BGC-O1 cluster region was specific to the *Oryza* lineage, we checked
222 whether flanking genomic regions of BGC-O1 were conserved or variable in different
223 lineages. We mapped representative high-quality assemblies from each lineage with the
224 reference genome assembly of the 70-15 strain from *Oryza* lineage to assess synteny at global

225 level. We found that BGC-O1 was located in the sub-telomeric region of chromosome 2
226 (NC_017850.1), and approximately 528 kb downstream of the *ACE1* gene cluster in the
227 reference strain 70-15. The macrosynteny analysis between 70-15 and GUY11, both strains
228 from *Oryza* lineage, showed conservation of ~134 kb upstream and ~117 kb downstream
229 flanking regions, along with the BGC-O1 cluster (Fig. 4A). The ~10 kb-long immediate
230 flanking regions were found to be swapped between the GUY11 and 70-15 genomes (Fig.
231 4A). Similarly, comparison between 70-15 and FR13 strains revealed a partial conservation
232 (~14 kb) of BGC-O1, with an ~9.5 kb region from BGC-O1 in 70-15 strain translocated
233 further downstream on the same contig in the FR13 strain (Fig. 4A). Further, while ~102 kb
234 upstream flanking region was syntenic in 70-15 and FR13, the downstream flanking region
235 showed a few structural rearrangements (Fig. 4A). In contrast, comparison with non-*Oryza*
236 lineages, like *Eleusine* and *Setaria*, showed a significant loss of synteny in the sub-telomeric
237 region of chromosome 2. While the upstream flanking region (~97 kb upstream of BGC-O1 in
238 70-15) was found to be syntenic to a corresponding region in MZ5-1-6, CD156 and US71, the
239 BGC-O1 cluster and downstream sequences were absent in the genomes of these lineages
240 (Fig. 4B).
241 Importantly, BGC-O1 did not show any similarity with any of the reference BGCs in MIBiG,
242 suggesting it to be a BGC, likely involved in production of a novel metabolite.
243
244 **BGC-O1 likely originates from a duplication event in the common ancestor of *P. oryzae***
245 **and *Colletotrichum eremochloae***
246 To understand the evolutionary history of BGC-O1, we searched for homologues of the
247 MGG_08236 PKS protein within *Pezizomycotina* from the MycoCosm repository (Grigoriev
248 et al., 2014). Only two orthologues could be retrieved from the fungus *Colletotrichum*

249 *eremochloae*. A phylogenetic analysis showed that the PKS 670826 (scaffold_178) from *C.*
250 *eremochloae* is an orthologue of MGG_08236 PKS, forming an outgroup to the *P. oryzae*
251 lineage (Fig. 5A). The other paralogue in *C. eremochloae*, 679399 (scaffold_5), belongs to a
252 clade that is restricted to the *Colletotrichum* genus and forms a sister clade to the
253 MGG_08236 PKS clade. Comparison of the genomic loci of both homologues in *C.*
254 *eremochloae* and BGC-O1 in *P. oryzae* showed that these two clusters shared the PKS and
255 two cytochrome P450 genes with BGC-O1 (Fig. 5B), while the orthologues of
256 methyltransferase and Co-A transferase genes were present elsewhere as single copies –
257 671186 and 576843 – on scaffold_185 and scaffold_10, respectively, in the *C. eremochloae*
258 genome. The presence of the two similar BGCs in *C. eremochloae* suggests that BGC-O1
259 likely originated from an ancestral duplication event. While *Pyricularia* and *Colletotrichum*
260 diverged ~250 MYA (calculated using TimeTree; Kumar et al., 2022), BGC-O1 is retained
261 only in *P. oryzae* and *C. eremochloae*, suggesting a role of respective host selection pressure
262 in its retention.
263
264 **BGC-O1 genes are expressed specifically during host invasion**
265 The presence of the PKS MGG_08236 gene was checked by PCR using genomic DNA of *P.*
266 *oryzae* strains from rice and finger millet host plants (Fig. 6A). The MGG_08236 gene was
267 present in all the *Oryza* strains studied, except for MOS3, which was identified as the only
268 *Oryza* lineage strain lacking the BGC-O1 based on the *in-silico* analysis. The MGG_08236
269 ORF was absent in all the *Eleusine* strains used as well as in the MOS1 and MOS4 strains,
270 which are placed outside of *Oryza* lineage in the phylogenetic analysis (Fig. 1B and 6A).
271 We then studied the expression of the PKS (MGG_08236) and three predicted tailoring genes
272 – methyl transferase (MGG_15107), CoA-transferase (MGG_15108) and cytochrome P450

273 (MGG_12496) of the BGC-O1 locus during different stages of infection, using RT-PCR.
274 Total RNA was isolated from fungal vegetative mycelia grown in complete medium, rice
275 leaves inoculated with *P. oryzae* and incubated for different time-points, and uninoculated
276 rice leaves, to assess the levels of transcripts of the aforementioned genes relative to those of
277 β-Tubulin as an internal control. While expression of the core PKS gene was undetected in
278 mycelium and at 12 hpi (pre-invasive stage), its transcripts started accumulating during
279 pathogenic development, with significantly elevated expression from 24 hpi till 96 hpi (Fig.
280 6B). The expression pattern of MGG_15107 and MGG_15108 tailoring genes partly
281 correlated with that of the PKS, (Fig. 6B). In contrast, MGG_12496 showed a different
282 expression pattern, where the transcript levels were similar during both vegetative growth and
283 host invasion (Fig. 6B), suggesting it is not co-regulated with other genes in the predicted
284 BGC-O1. This result shows that the MGG_08236 PKS gene is specifically expressed during
285 pathogenesis on rice and potentially has a key role to play during host colonization.
286 Altogether, our *in-silico* analyses identified a novel PKS gene cluster in the *Oryza*- and
287 *Eragrostis*-specific lineages, which likely played a key role in shaping specialization of the
288 blast fungus to rice and weeping lovegrass host plants.
289
290 **Discussion**
291
292 **Population genomics identifies BGCs with potential roles in virulence and host**
293 **specialization in *P. oryzae***
294 We identified three lineage-specific BGCs in the blast fungal pathogen *P. oryzae* using a
295 population genomics approach. While two of them appeared to encode non-functional
296 enzymes, the *Oryza* and *Eragrostis*-specific BGC, named BGC-O1, appears functional and is

297 present in almost all the genomes from *Oryza* (23 out of 24) and *Eragrostis* (1 out of 1)
298 lineages studied here. Our population-genomics-based finding of the *Oryza* lineage-specific
299 BGC (BGC-O1) is supported by gene expression analyses. Indeed, we found that the *Oryza*-
300 lineage-specific PKS (MGG_08236) transcript accumulated specifically during penetration
301 and colonization of the rice host. Recent transcriptomics-based studies have shown that the
302 expression of the PKS encoded in BGC-O1 (MGG_08236) and neighboring tailoring genes
303 (methyl transferase, MGG_15107 and Co-A transferase, MGG_15108) was induced during
304 the initial biotrophic colonization stage of blast disease (Jeon et al., 2020; Yan et al., 2023).
305 Importantly, the expression of MGG_08236, along with the other pathogenesis-related genes
306 such as the SM gene cluster *ACE1* and protein effectors SLP2, BAS2, BAS3 and AVR-Pi9,
307 was recently found to be under the control of the bZIP transcription factor Bip1 (Lambou et
308 al., 2024). Bip1 is found to be regulating expression of a specific set of genes involved in
309 early biotrophic stage of blast infection (Lambou et al., 2024). These findings strongly
310 suggest that the SM produced by BGC-O1 could exhibit an effector-like function. Many plant
311 fungal pathogens such as *Colletotrichum higginsianum, Fusarium graminearum,*
312 *Zymoseptoria tritici*, and *P. oryzae* are known to produce a number of SMs during
313 pathogenesis, especially during host penetration and colonization (Collemare, Billard, et al.,
314 2008; Dallery et al., 2017; Harris et al., 2016; Jeon et al., 2020; Palma-Guerrero et al., 2017;
315 Patkar et al., 2015; Rudd et al., 2015; Yan et al., 2023). To study if the BGC-O1 has any role
316 in virulence in a host-specific manner, deletion of the *PKS* gene (MGG_08236) was attempted
317 in an *Oryza*-specific isolate. Despite using different approaches and a number of attempts,
318 generation of a deletion mutant has been unsuccessful so far, possibly due to its presence in
319 the sub-telomeric region of chromosome 2 of the reference strain 70-15. A similar difficulty
320 was faced in generating deletion mutant at the *ACE1* locus (Collemare, Pianfetti, et al., 2008).

321 Nonetheless, the MOS3 strain from *Oryza* lineage, which lacks the BGC-O1, failed to infect
322 rice host as effectively as B157, MOS2 or MOS6 (Fig. 6A; Supplementary Fig. S2A). This
323 could possibly explain the key role of BGC-O1 in specialization to rice host.
324 While only three BGCs were present in host-specific lineages, most of the other BGCs were
325 found in all lineages. However, such apparently conserved BGCs can show variation in their
326 tailoring gene content. Such differences could result in the production of distinct SMs with
327 potential effector function in a host specific manner. Alternatively, conservation of BGCs in
328 different lineages could indicate a key role in virulence on cereals. Thus, analyses
329 investigating variations among conserved SM-producing BGCs across different *P. oryzae*
330 lineages could be useful in identifying the likely diversity in the SMs produced and their
331 association with specific hosts.
332
333 **Conservation of BGC-O1 in an unstable genomic context**
334 We found that the *Oryza*-specific cluster BGC-O1 is located in the sub-telomeric region on
335 the chromosome 2 (NC_017850.1) of the reference strain 70-15. While the genomic regions
336 covering the BGC-O1 and its flanking sequences were highly syntenic in strains from the
337 *Oryza* lineage, only the upstream flanking region of this locus was found conserved in all the
338 other lineages. The chromosome ends tend to have substantially higher levels of
339 polymorphism because they frequently undergo rearrangements due to the presence of AT-
340 rich repeats and transposable elements (Farman & Kim, 2005; Rahnama et al., 2020; Starnes
341 et al., 2012). In the absence of sexual reproduction, asexually propagating pathogens likely
342 utilize chromosomal rearrangements as one of the mechanisms of host-specialization as
343 shown in *Verticillium dahliae* (Jonge et al., 2013). Similarly, the regions adjacent to a
344 telomere in *P. oryzae* are reported to be highly polymorphic and enriched with genes involved

345 in interaction with its host plants (Rahnama et al., 2021). Gain and/or loss of effector genes,
346 lineage-specific gene families and chromosomal rearrangements are likely the major
347 evolutionary mechanisms involved in such host specificity and adaptation of *P. oryzae*
348 (Chiapello et al., 2015; Chuma et al., 2011; Gómez Luciano et al., 2019; Jonge et al., 2013;
349 Yoshida et al., 2016). Given that BGC-O1 is also flanked by transposons in most strains of
350 the *Oryza* lineage of *P. oryzae* (Fig. 3), we hypothesize that genomic alterations, most likely
351 through deletions, may have resulted in the loss of the BGC in other host-specialized lineages.
352 We further found that BGC-O1 is located on a mini-chromosome (UEMA03000009.1) in the
353 FR13 isolate, which also carries the *ACE1* BGC. Large-scale genomic rearrangements around
354 the loci of several virulence-related genes (*ACE1* and *AVR-Pik*) likely led to the emergence of
355 supernumerary mini-chromosome in the rice isolate FR-13, facilitating the adaptive evolution
356 of the blast fungus (Langner et al., 2021). Thus, retention of BGC-O1 in *Oryza* and *Eragrostis*
357 lineages, despite its localization in unstable sub-telomeric regions, suggests a significant role
358 of host selection pressure in its conservation therein. The most likely selection pressure to
359 retain BGC-O1 relates to the ability to successfully infect a host, which is also indicated by
360 the specific expression profile during infection. The presence of homologous BGCs in *C.*
361 *eremochloae*, the causal agent of anthracnose disease on centipede-grass turf in southern
362 United States (Crouch & Tomaso-Peterson, 2012), suggests a particular function for BGC-O1
363 in infecting certain cereals only (*Oryza*, *Eragrostis*, *Eremochloa*). Further investigations are
364 needed to determine if the *C. eremochloae* BGC is expressed during infection and whether it
365 produces the same metabolite as BGC-O1 in *P. oryzae*.
366
367 **Conclusions**
368

369 Our findings highlight the importance of population genomics-based studies in identifying
370 secondary metabolite BGCs and the corresponding genomic rearrangements, likely driven by
371 the host selection pressure, which could lead to a host-specialized lineage of the blast fungal
372 pathogen.
373
374 **Methods**
375
376 **Fungal strains and culture conditions**
377 We isolated 15 field strains of *P. oryzae* from different geographic locations in India and from
378 three different host plants – rice (*Oryza sativa*), finger millet *(Eleusine coracana*) and foxtail
379 millet (*Setaria italica*). Infected tissues with blast lesions were collected and used for single
380 spore isolation. Leaf tissues with blast disease lesions were surface sterilized using 70%
381 ethanol and 1% sodium hypochlorite, followed by three successive washes with sterile
382 distilled water. Surface-sterilized leaf tissues were incubated under micro-humid conditions
383 maintained in a Petri dish for 24-48 h to induce sporulation. Spores were suspended in sterile
384 water and spread evenly on 2% water agar plate. Single germinating spores were picked up
385 under a microscope, and inoculated on Prune Agar (PA: 1 g/L yeast extract, 2.5 g/L lactose,
386 2.5 g/L sucrose, 0.04% prune juice, pH 6.5; Soundararajan et al., 2004) plates and incubated
387 at 28 °C. Vegetative growth of the fungus on PA plates was continued for 10 days at 28 °C,
388 with initial 3-day incubation under dark conditions, followed by 7-day incubation under
389 constant illumination for conidiation. Genomic DNA was extracted by grinding in liquid
390 nitrogen the fungal biomass obtained from vegetative culture grown in a complete medium
391 (CM: 6 g/L yeast extract, 6 g/L casein enzyme hydrolysate, 10 g/L sucrose) for ~3 days at 28
392 °C, followed by the standard protocols as described earlier (Dellaporta et al., 1983).

393

394 **Genome sequencing and assemblies**

395 Newly isolated strains were sequenced for whole genome using a paired-end sequencing
396 approach at >50X depth on Illumina HiSeq2500 platform at AgriGenome Labs Pvt. Ltd.,
397 India. Short raw reads were processed using Trimmomatic v0.38 at a threshold for the
398 minimum read length of 80 bp for paired-end reads (parameters PE, Leading:10, Trailing:10,
399 Slidingwindow:4:20, Minlen:80; Bolger et al., 2014). *De novo* sequence assemblies were
400 constructed using CLC Genomics Workbench v11.0 with default parameters (Word size:23,
401 Bubble Size:50, Minimum contig length:500, Mismatch cost:2, Insertion cost:3, Deletion
402 cost:3, Length fraction:0.5, Similarity fraction:0.8). Additionally, we used publicly available
403 genome sequences of *P. oryzae* strains from NCBI (Supplementary table S1). The overall
404 quality of each genome assembly was evaluated using BUSCO v5.2.2 (Simão et al., 2015)
405 with the Sordariomycetes dataset. We carried out gene predictions on all the assemblies using
406 Augustus v3.3.3 (Stanke et al., 2006) with Magnaporthe_grisea as a species model.

407

408 **Construction of species tree**

409 2655 BUSCO proteins conserved in 68 *P. oryzae* strains were retrieved from the BUSCO
410 analysis and aligned using Mafft v7.475 (parameters -reorder; Katoh et al., 2002). TrimAL
411 v1.4.1 (parameters -automated1; Capella-Gutiérrez et al., 2009) was used to remove poorly
412 aligned regions (Supplementary dataset S1, S2). A maximum likelihood tree was generated
413 using IQ-TREE v2.1.2 (Minh et al., 2020) with partition models (Chernomor et al., 2016;
414 Lanfear et al., 2014), model finder (Kalyaanamoorthy et al., 2017) and ultrafast bootstrap
415 (Hoang et al., 2018; parameters -m MF -p partition.nex -bb 1000) (Supplementary dataset S3,
416 S4). Similarly, a species tree including 3 *Pyricularia grisea* and 68 *P. oryzae* strains was

417 generated using a total of 2557 BUSCO proteins (Supplementary dataset S5-S7). Both trees
418 were visualized and annotated using iTOL (Letunic & Bork, 2021).
419
420 **Prediction of BGCs and similarity network analysis**
421 BGCs were predicted using antiSMASH v6.0.1 (Blin et al., 2021; parameters -taxon fungi -
422 minimal -cluster_hmmer -pfam2go). All the predicted BGCs and reference fungal BGCs from
423 the MIBiG v2.1 (Kautsar et al., 2019) repository were included to perform a similarity
424 network analysis using BiG-SCAPE v1.1.0 (Navarro-Muñoz et al., 2019) with glocal mode
425 and with different cut-off values (parameters –include_singletons –mix –no_classify –clans-
426 off –cutoffs 0.3 0.4 0.5 0.7). A cut-off value of 0.5 was found to be appropriate, as the
427 relevant BGCs showed similarity with the reference BGCs from MIBiG known for
428 metabolites such as DHN (melanin), epipyriculol, alternapyrone, squalestatin S1 and
429 cytochalasans. The network files were visualized with Cytoscape v3.8.2 (Shannon et al.,
430 2003). Visualization of BGC conservation was done with Clinker (Gilchrist & Chooi, 2021).
431 Gene models belonging to BGC-O1 family were manually curated (Supplementary dataset
432 S8).
433
434 **Statistics for natural selection**
435 To test for natural selection, 40 SM core biosynthetic genes shared by at least ten isolates
436 from each host-specific lineage (*Oryza*, *Eleusine* and *Triticum*) were used to calculate
437 polymorphism and divergence (Supplementary Table S4). For each gene, the nucleotide
438 coding region in the different strains were aligned using Mafft v7.475 (parameters -reorder;
439 Katoh et al., 2002). DnaSP v6 (Rozas et al., 2017) was used to calculate the levels of

440 polymorphism within population (Pi(a)/Pi(s)) and divergence between the populations
441 (Ka/Ks).
442
443 **Synteny analysis**
444 To identify the syntenic genomic regions between any genome assembly and the reference
445 70-15 strain assembly, global alignments were generated using nucmer (parameters –c 100 --
446 maxmatch) program from MUMMER v3.23 package (Kurtz et al., 2004). Alignments were
447 further filtered using delta-filter utility with length >10 kb and percent identity >80%
448 (parameters -l 10000 -i 80) to retrieve continuous syntenic blocks. The show-coords utility
449 was used to extract alignment coordinates in tabular format and the plots were generated in R
450 using KaryoploteR package (Gel & Serra, 2017).
451
452 **Core gene phylogeny**
453 Homologs of MGG_08236 were identified in *Pezizomycotina* from the Joint Genome Institute
454 MycoCosm repository (Grigoriev et al., 2014) using BLASTp. The resulting Blast hits were
455 filtered for top 3 hits of each species. Amino acid sequences were aligned using MAFFT
456 v7.475 (Katoh et al., 2002) and poorly aligned regions were removed with TrimAl v1.4.1
457 (Capella-Gutiérrez et al., 2009). A phylogenetic tree was constructed using Fasttree v2.1.11
458 (parameters -lg; Price et al., 2010) to identify orthologues and closest paralogues. The
459 identified orthologous protein sequences were used to build a phylogenetic tree using IQ-
460 TREE v2.1.2 (Minh et al., 2020) with LG substitution model and ultrafast bootstrap (Hoang et
461 al., 2018), and the SH-like approximate likelihood-ratio test (Guindon et al., 2010) for branch
462 support (parameters -mset LG -bb 1000 -alrt 1000) (Supplementary dataset S9-S11). The tree
463 was visualized and annotated using iTOL (Letunic & Bork, 2021).

464

465 **Whole-plant infection assay**

466 Conidia were harvested as per the protocol described earlier (Patkar et al., 2012) from
467 different strains collected in India. Whole-plant infection assay was carried out by spraying 10
468 mL spore suspension (~ 10^5 conidia/mL) containing 0.05% w/v gelatin onto ~ 4-week-old
469 host plants, rice cv. CO-39 and finger millet cv. GN-4, and ~3-week-old foxtail millet cv.
470 SIA-3088 plants, followed by incubation at 28–30 °C under humid conditions, initially for 24
471 h in the dark and then for 4–6 days under 14 h light and 10 h dark cycles. Development of
472 disease symptoms was monitored regularly during the entire incubation period and recorded
473 around 5-8 days post inoculation depending on the appearance of lesions on the leaves. The
474 infection assays were carried out with at least three biological replicates.

475

476 **Gene expression analysis by semi-quantitative RT-PCR**

477 The expression profiles of four genes (MGG_08236, MGG_15107, MGG_15108 and
478 MGG_12496) were studied during different stages of infection on ~ 4-week-old rice plants
479 (blast susceptible variety PB-1509). Briefly, 20 µL conidial suspension (~10^5 conidia/mL
480 with 0.01% Tween-20) of B157 strain from *Oryza* lineage was drop-inoculated on to the
481 surface-sterilized detached leaf blades placed on water agar plates containing 2 µg/mL
482 Kinetin, followed by incubation under dark (10 h) and light (14 h) cycles at 25 °C. Samples
483 were collected by excising inoculated portions on the leaf blades, at 12-, 24-, 48-, 72- and 96-
484 hours post inoculation (hpi). Three-day-old vegetative mycelia, grown in liquid CM, was used
485 as a control condition. A sample from mock-inoculation (leaf blades inoculated with only
486 0.01% Tween-20) was used as another experimental control to check any non-specific
487 amplification during RT-PCR. Total RNA was extracted from all samples using TRIzol®

488 reagent (Invitrogen, USA) as per the manufacturer's instructions. Two μg of total RNA each
489 was used for cDNA synthesis using iScript™ cDNA Synthesis Kit (Bio-Rad, USA).
490 Oligonucleotide primers used for RT-PCR for each gene are listed in Supplementary Table
491 S5. Optimized thermal cycling conditions for RT-PCR were as follows: initial denaturation
492 step at 95 °C for 5 min, followed by 30 cycling reactions each at 95 °C (denaturation step) for
493 30 s, 60 °C (annealing step) for 30 s and 72 °C (extension step); and the final extension step at
494 72 °C for 5 min. The *MGG_08236* ORF was amplified from the genomic DNA of *P. oryzae*
495 strains from different lineages using the same thermal cycling conditions as above, except for
496 the extension step, which was set at 1 min in each cycle.
497

Abbreviations

ACE1	Avirulene Conferring Enzyme1
AVR	Avirulence
BGC	Biosynthetic Gene Cluster
BGC-O1	Biosynthetic Gene Cluster specific to *Oryza* lineage - 1
BGC-O2	Biosynthetic Gene Cluster specific to *Oryza* lineage - 2
BGC-TLE	Biosynthetic Gene Cluster specific to *Triticum*, *Lolium* and *Eleusine* lineages
BiG-SCAPE	Biosynthetic Gene Similarity Clustering and Prospecting Engine
BUSCO	Benchmarking Universal Single-Copy Orthologs
CM	Complete Media
GCF	Gene Cluster Family
hpi	hours post inoculation
HST	Host Selective Toxin
MIBiG	Minimum Information about a Biosynthetic Gene cluster
NCBI	National Centre for Biotechnology Information
NRPS	NonRibosomal Peptide Synthetase
ORF	Open Reading Frame
PA	Prune Agar
PCR	Polymerase Chain Reaction
PKS	PolyKetide Synthase
RT-PCR	Reverse Transcriptase Polymerase Chain Reaction
SM	Secondary Metabolites
TC	Terpene Cyclases

Declarations

Ethics approval and consent to participate

Not applicable

Consent for publication

Not applicable

Availability of data and materials

Raw sequence data for the newly sequenced Indian strains under this study have been made accessible at SRA database under the BioProject ID PRJNA973860. All datasets generated for this study are included in the article/Supplementary Material. All the Supplementary Datasets can be accessed through a link: https://drive.google.com/drive/folders/18Uw6663e87ZyXRDEO-2aJpcoNuB7padZ?usp=share_link

Competing interests

The authors declare that they have no competing interests.

Funding

Prof. Bharat Chattoo acquired the grant (BT/PR6949/AGIII/103/862/2012) from DBT, GoI. KM was supported by the DBT (GoI)-funded grant (BT/PR6949/AGIII/103/862/2012) and partly by the intramural University Research Scholarship from The M. S. University of Baroda. KM received EMBO - Scientific Exchange Grant (SEG no. 8866) to conduct part of

525 this work at the Westerdijk Institute, The Netherlands. RP was awarded by SERB, GoI
526 (EMR/2017/005303) and the Seed Grant, IIT Bombay.
527

528 **Authors' contributions**

529 KM collected samples and contributed to the isolation of the Indian strains of blast fungus and
530 phenotyping experiments. KM conducted formal analyses on diversity in BGCs, JC and JCN-
531 M helped with the investigation of the analyses. KM, RP and JC conducted image analyses
532 and statistical analyses. JCN-M provided important in-house scripts for similarity network
533 analysis. SB helped KM with the gene expression analysis. KM wrote the original draft of the
534 manuscript. All authors contributed to the review and editing of the manuscript. KM, RP and
535 JC designed the study. RP provided the resources for the study. RP and JC supervised the
536 study.
537

538 **Acknowledgements**

539 We acknowledge late Prof. Bharat B. Chattoo for his guidance and providing sophisticated
540 laboratory facility at the Bharat Chattoo Genome Research Centre (BCGRC). We also fondly
541 remember late Dr. Johannes Manjrekar for the useful scientific discussions during this work.
542 We thank Dr. Malali Gowda and Dr. T. R. Sharma for providing blast-infected tissues for
543 some of the isolates used in this study. We thank the BCGRC group at MSU for useful
544 discussions. We thank Dr. Noppol Kobmoo (Biotec) for his useful insights on natural
545 selection and population genetics analyses.
546 Some sequence data were produced by the US Department of Energy (DOE) Joint Genome
547 Institute (https://www.jgi.doe.gov/) in collaboration with the user community. We especially
548 thank Dr. Rytas Vilgalys and Dr. Francis Martin for using the *Diaporthaceae* sp. PMI_573

549 genome generated within the framework of the 1000 Fungal Genome projects (CSP 1974).
550 We also thank Dr. Riccardo Baroncelli for letting us use the genomes of *Colletotrichum*
551 *melonis* CBS 134730 (Colme1) and *Colletotrichum tamarilloi* CBS 129955 (Colta1).
552

553 **Benefit-sharing section statement**

554 A research collaboration established with scientists from Westerdijk Fungal Biodiversity
555 Institute, The Netherlands, was helpful in *in-silico* analyses of the secondary metabolism
556 related gene clusters in the blast fungal pathogen. All collaborators are included as co-authors.
557 The results of research, addressing a priority concern, will be shared with the broader
558 scientific community.
559

References

Asuke, S., Tanaka, M., Hyon, G.-S., Inoue, Y., Vy, T. T. P., Niwamoto, D., Nakayashiki, H., & Tosa, Y. (2020). Evolution of an *Eleusine* -Specific Subgroup of *Pyricularia oryzae* Through a Gain of an Avirulence Gene. *Molecular Plant-Microbe Interactions®*, *33*(2), 153–165. https://doi.org/10.1094/MPMI-03-19-0083-R

Blin, K., Shaw, S., Kloosterman, A. M., Charlop-Powers, Z., Van Wezel, G. P., Medema, M. H., & Weber, T. (2021). antiSMASH 6.0: Improving cluster detection and comparison capabilities. *Nucleic Acids Research*, *49*(W1), W29–W35. https://doi.org/10.1093/nar/gkab335

Böhnert, H. U., Fudal, I., Dioh, W., Tharreau, D., Notteghem, J. L., & Lebrun, M. H. (2004). A putative polyketide synthase/peptide synthetase from Magnaporthe grisea signals pathogen attack to resistant rice. *Plant Cell*, *16*(9), 2499–2513. https://doi.org/10.1105/tpc.104.022715

Bolger, A. M., Lohse, M., & Usadel, B. (2014). Trimmomatic: A flexible trimmer for Illumina sequence data. *Bioinformatics (Oxford, England)*, *30*(15), 2114–2120. https://doi.org/10.1093/bioinformatics/btu170

Brunner, P. C., & McDonald, B. A. (2018). Evolutionary analyses of the avirulence effector AvrStb6 in global populations of *Zymoseptoria tritici* identify candidate amino acids involved in recognition. *Molecular Plant Pathology*, *19*(8), 1836–1846. https://doi.org/10.1111/mpp.12662

Capella-Gutiérrez, S., Silla-Martínez, J. M., & Gabaldón, T. (2009). trimAl: A tool for automated alignment trimming in large-scale phylogenetic analyses. *Bioinformatics*, *25*(15), 1972–1973. https://doi.org/10.1093/bioinformatics/btp348

Chen, S., & Qiang, S. (2017). Recent advances in tenuazonic acid as a potential herbicide. *Pesticide Biochemistry and Physiology*, *143*, 252–257. https://doi.org/10.1016/j.pestbp.2017.01.003

Chernomor, O., Von Haeseler, A., & Minh, B. Q. (2016). Terrace Aware Data Structure for Phylogenomic Inference from Supermatrices. *Systematic Biology*, *65*(6), 997–1008. https://doi.org/10.1093/SYSBIO/SYW037

Chiapello, H., Mallet, L., Guérin, C., Aguileta, G., Amselem, J., Kroj, T., Ortega-Abboud, E., Lebrun, M.-H., Henrissat, B., Gendrault, A., Rodolphe, F., Tharreau, D., & Fournier, E. (2015). Deciphering Genome Content and Evolutionary Relationships of Isolates from the Fungus Magnaporthe oryzae Attacking Different Host Plants. *Genome Biology and Evolution*, *7*(10), 2896–2912. https://doi.org/10.1093/gbe/evv187

Chuma, I., Isobe, C., Hotta, Y., Ibaragi, K., Futamata, N., Kusaba, M., Yoshida, K., Terauchi, R., Fujita, Y., Nakayashiki, H., Valent, B., & Tosa, Y. (2011). Multiple translocation of the AVR-Pita effector gene among chromosomes of the rice blast fungus Magnaporthe oryzae and related species. *PLoS Pathogens*, *7*(7), e1002147. https://doi.org/10.1371/journal.ppat.1002147

Chumley, F. G., & Valent, B. (1990). Genetic Analysis of Melanin-Deficient, Nonpathogenic Mutants of Magnaporthe grisea. *Molecular Plant-Microbe Interactions*, *3*(3), 135. https://doi.org/10.1094/MPMI-3-135

Collemare, J., Billard, A., Böhnert, H. U., & Lebrun, M.-H. (2008). Biosynthesis of secondary metabolites in the rice blast fungus Magnaporthe grisea: The role of hybrid PKS-NRPS in pathogenicity. *Mycological Research*, *112*(2), 207–215. https://doi.org/10.1016/j.mycres.2007.08.003

Collemare, J., O'Connell, R., & Lebrun, M. H. (2019). Nonproteinaceous effectors: The terra incognita of plant–fungal interactions. *New Phytologist*, *223*(2), 590–596. https://doi.org/10.1111/nph.15785

Collemare, J., Pianfetti, M., Houlle, A.-E., Morin, D., Camborde, L., Gagey, M.-J., Barbisan, C., Fudal, I., Lebrun, M.-H., & Böhnert, H. U. (2008). *Magnaporthe grisea* avirulence gene *ACE1* belongs to an infection-specific gene cluster involved in secondary metabolism. *New Phytologist*, *179*(1), 196–208. https://doi.org/10.1111/j.1469-8137.2008.02459.x

Crouch, J. A., & Tomaso-Peterson, M. (2012). Anthracnose disease of centipedegrass turf caused by Colletotrichum eremochloae, a new fungal species closely related to Colletotrichum sublineola. *Mycologia*, *104*(5), 1085–1096. https://doi.org/10.3852/11-317

Dallery, J.-F., Lapalu, N., Zampounis, A., Pigné, S., Luyten, I., Amselem, J., Wittenberg, A. H. J., Zhou, S., de Queiroz, M. V., Robin, G. P., Auger, A., Hainaut, M., Henrissat, B., Kim, K.-T., Lee, Y.-H., Lespinet, O., Schwartz, D. C., Thon, M. R., & O'Connell, R. J. (2017). Gapless genome assembly of Colletotrichum higginsianum reveals chromosome structure and association of transposable elements with secondary metabolite gene clusters. *BMC Genomics*, *18*(1), 667. https://doi.org/10.1186/s12864-017-4083-x

Dellaporta, S. L., Wood, J., & Hicks, J. B. (1983). A plant DNA minipreparation: Version II. *Plant Molecular Biology Reporter*, *1*(4), 19–21. https://doi.org/10.1007/BF02712670

Ebbole, D. J. (2007). Magnaporthe as a model for understanding host-pathogen interactions. *Annual Review of Phytopathology*, *45*, 437–456. https://doi.org/10.1146/annurev.phyto.45.062806.094346

Farman, M. L., & Kim, Y. S. (2005). Telomere hypervariability in Magnaporthe oryzae. *Molecular Plant Pathology*, *6*(3), 287–298. https://doi.org/10.1111/J.1364-3703.2005.00285.X

Fudal, I., Collemare, J., Böhnert, H. U., Melayah, D., & Lebrun, M.-H. (2007). Expression of Magnaporthe grisea Avirulence Gene ACE1 Is Connected to the Initiation of Appressorium-Mediated Penetration. *Eukaryotic Cell*, *6*(3), 546–554. https://doi.org/10.1128/EC.00330-05

Gel, B., & Serra, E. (2017). karyoploteR: an R/Bioconductor package to plot customizable genomes displaying arbitrary data. *Bioinformatics*, *33*(19), 3088–3090. https://doi.org/10.1093/BIOINFORMATICS/BTX346

Gilchrist, C. L. M., & Chooi, Y. H. (2021). clinker & clustermap.js: Automatic generation of gene cluster comparison figures. *Bioinformatics*, *37*(16), 2473–2475. https://doi.org/10.1093/BIOINFORMATICS/BTAB007

Giraud, T., Gladieux, P., & Gavrilets, S. (2010). Linking the emergence of fungal plant diseases with ecological speciation. *Trends in Ecology & Evolution*, *25*(7), 387–395. https://doi.org/10.1016/J.TREE.2010.03.006

Gladieux, P., Condon, B., Ravel, S., Soanes, D., Maciel, J. L. N., Nhani, A., Chen, L., Terauchi, R., Lebrun, M., Tharreau, D., Mitchell, T., Pedley, K. F., Valent, B., Talbot, N. J., Farman, M., & Fournier, E. (2018). Gene Flow between Divergent Cereal- and Grass-Specific Lineages of the Rice Blast Fungus Magnaporthe oryzae. *mBio*, *9*(1), 1–19. https://doi.org/10.1128/mBio.01219-17

Gladieux, P., Ropars, J., Badouin, H., Branca, A., Aguileta, G., De Vienne, D. M., Rodríguez De La Vega, R. C., Branco, S., & Giraud, T. (2014). Fungal evolutionary genomics

provides insight into the mechanisms of adaptive divergence in eukaryotes. *Molecular Ecology*, *23*(4), 753–773. https://doi.org/10.1111/mec.12631

Gómez Luciano, L. B., Tsai, I. J., Chuma, I., Tosa, Y., Chen, Y. H., Li, J. Y., Li, M. Y., Lu, M. Y. J., Nakayashiki, H., & Li, W. H. (2019). Blast Fungal Genomes Show Frequent Chromosomal Changes, Gene Gains and Losses, and Effector Gene Turnover. *Molecular Biology and Evolution*, *36*(6), 1148–1161. https://doi.org/10.1093/molbev/msz045

Grigoriev, I. V., Nikitin, R., Haridas, S., Kuo, A., Ohm, R., Otillar, R., Riley, R., Salamov, A., Zhao, X., Korzeniewski, F., Smirnova, T., Nordberg, H., Dubchak, I., & Shabalov, I. (2014). MycoCosm portal: Gearing up for 1000 fungal genomes. *Nucleic Acids Research*, *42*(D1), D699–D704. https://doi.org/10.1093/NAR/GKT1183

Guindon, S., Dufayard, J. F., Lefort, V., Anisimova, M., Hordijk, W., & Gascuel, O. (2010). New Algorithms and Methods to Estimate Maximum-Likelihood Phylogenies: Assessing the Performance of PhyML 3.0. *Systematic Biology*, *59*(3), 307–321. https://doi.org/10.1093/SYSBIO/SYQ010

Harris, L. J., Balcerzak, M., Johnston, A., Schneiderman, D., & Ouellet, T. (2016). Host-preferential Fusarium graminearum gene expression during infection of wheat, barley, and maize. *Fungal Biology*, *120*(1), 111–123. https://doi.org/10.1016/j.funbio.2015.10.010

Hartmann, F. E., McDonald, B. A., & Croll, D. (2018). Genome-wide evidence for divergent selection between populations of a major agricultural pathogen. *Molecular Ecology*, *27*(12), 2725–2741. https://doi.org/10.1111/mec.14711

Hoang, D. T., Chernomor, O., Von Haeseler, A., Minh, B. Q., & Vinh, L. S. (2018). UFBoot2: Improving the Ultrafast Bootstrap Approximation. *Molecular Biology and Evolution*, *35*(2), 518–522. https://doi.org/10.1093/MOLBEV/MSX281

Inoue, Y., Vy, T. T. P., Yoshida, K., Asano, H., Mitsuoka, C., Asuke, S., Anh, V. L., Cumagun, C. J. R., Chuma, I., Terauchi, R., Kato, K., Mitchell, T., Valent, B., Farman, M., & Tosa, Y. (2017). Evolution of the wheat blast fungus through functional losses in a host specificity determinant. *Science (New York, N.Y.)*, *357*(6346), 80–83. https://doi.org/10.1126/science.aam9654

Izumi, Y., Ohtani, K., Miyamoto, Y., Masunaka, A., Fukumoto, T., Gomi, K., Tada, Y., Ichimura, K., Peever, T. L., & Akimitsu, K. (2012). A Polyketide Synthase Gene, *ACRTS2* , Is Responsible for Biosynthesis of Host-Selective ACR-Toxin in the Rough Lemon Pathotype of *Alternaria alternata*. *Molecular Plant-Microbe Interactions®*, *25*(11), 1419–1429. https://doi.org/10.1094/MPMI-06-12-0155-R

Jacob, S., Grötsch, T., Foster, A. J., Schüffler, A., Rieger, P. H., Sandjo, L. P., Liermann, J. C., Opatz, T., & Thines, E. (2017). Unravelling the biosynthesis of pyriculol in the rice blast fungus magnaporthe oryzae. *Microbiology (United Kingdom)*, *163*(4), 541–553. https://doi.org/10.1099/mic.0.000396

Jeon, J., Lee, G. W., Kim, K. T., Park, S. Y., Kim, S., Kwon, S., Huh, A., Chung, H., Lee, D. Y., Kim, C. Y., & Lee, Y. H. (2020). Transcriptome profiling of the rice blast fungus magnaporthe oryzae and its host oryza sativa during infection. *Molecular Plant-Microbe Interactions*, *33*(2), 141–144. https://doi.org/10.1094/MPMI-07-19-0207-A

Jonge, R. de, Bolton, M., Kombrink, A., Berg, G. V. D. van den, Yadeta, K. A., & Thomma, B. (2013). Extensive chromosomal reshuffling drives evolution of virulence in an asexual pathogen. *Genome Research*. https://doi.org/10.1101/GR.152660.112

Kalyaanamoorthy, S., Minh, B. Q., Wong, T. K. F., Von Haeseler, A., & Jermiin, L. S. (2017). ModelFinder: Fast model selection for accurate phylogenetic estimates. *Nature Methods 2017 14:6*, *14*(6), 587–589. https://doi.org/10.1038/nmeth.4285

Katoh, K., Misawa, K., Kuma, K. I., & Miyata, T. (2002). MAFFT: a novel method for rapid multiple sequence alignment based on fast Fourier transform. *Nucleic Acids Research*, *30*(14), 3059–3066. https://doi.org/10.1093/NAR/GKF436

Kautsar, S. A., Blin, K., Shaw, S., Navarro-Muñoz, J. C., Terlouw, B. R., van der Hooft, J. J. J., van Santen, J. A., Tracanna, V., Suarez Duran, H. G., Pascal Andreu, V., Selem-Mojica, N., Alanjary, M., Robinson, S. L., Lund, G., Epstein, S. C., Sisto, A. C., Charkoudian, L. K., Collemare, J., Linington, R. G., … Medema, M. H. (2019). MIBiG 2.0: A repository for biosynthetic gene clusters of known function. *Nucleic Acids Research*. https://doi.org/10.1093/nar/gkz882

Kumar, S., Suleski, M., Craig, J. M., Kasprowicz, A. E., Sanderford, M., Li, M., Stecher, G., & Hedges, S. B. (2022). TimeTree 5: An Expanded Resource for Species Divergence Times. *Molecular Biology and Evolution*, *39*(8), msac174. https://doi.org/10.1093/molbev/msac174

Kurtz, S., Phillippy, A., Delcher, A. L., Smoot, M., Shumway, M., Antonescu, C., & Salzberg, S. L. (2004). Versatile and open software for comparing large genomes. *Genome Biology*, *5*(2), R12. https://doi.org/10.1186/gb-2004-5-2-r12

Lambou, K., Tag, A., Lassagne, A., Collemare, J., Clergeot, P.-H., Barbisan, C., Perret, P., Tharreau, D., Millazo, J., Chartier, E., Vries, R. P. D., Hirsch, J., Morel, J.-B., Beffa, R., Kroj, T., Thomas, T., & Lebrun, M.-H. (2024). The bZIP transcription factor BIP1 of the rice blast fungus is essential for infection and regulates a specific set of appressorium genes. *PLOS Pathogens*, *20*(1), e1011945. https://doi.org/10.1371/journal.ppat.1011945

Lanfear, R., Calcott, B., Kainer, D., Mayer, C., & Stamatakis, A. (2014). Selecting optimal partitioning schemes for phylogenomic datasets. *BMC Evolutionary Biology*, *14*(1), 1–14. https://doi.org/10.1186/1471-2148-14-82

Langner, T., Harant, A., Gomez-Luciano, L. B., Shrestha, R. K., Malmgren, A., Latorre, S. M., Burbano, H. A., Win, J., & Kamoun, S. (2021). Genomic rearrangements generate hypervariable mini-chromosomes in host-specific isolates of the blast fungus. *PLOS Genetics*, *17*(2), e1009386. https://doi.org/10.1371/journal.pgen.1009386

Letunic, I., & Bork, P. (2021). Interactive Tree Of Life (iTOL) v5: An online tool for phylogenetic tree display and annotation. *Nucleic Acids Research*, *49*(W1), W293–W296. https://doi.org/10.1093/NAR/GKAB301

Lim, S. M., & Hooker, A. L. (1971). Southern Corn Leaf Blight: Genetic Control of Pathogenicity and Toxin Production in Race T and Race O of *Cochliobolus heterostrophus*. *Genetics*, *69*(1), 115–117. https://doi.org/10.1093/genetics/69.1.115

Minh, B. Q., Schmidt, H. A., Chernomor, O., Schrempf, D., Woodhams, M. D., Von Haeseler, A., Lanfear, R., & Teeling, E. (2020). IQ-TREE 2: New Models and Efficient Methods for Phylogenetic Inference in the Genomic Era. *Molecular Biology and Evolution*, *37*(5), 1530–1534. https://doi.org/10.1093/molbev/msaa015

Navarro-Muñoz, J. C., Selem-Mojica, N., Mullowney, M. W., Kautsar, S. A., Tryon, J. H., Parkinson, E. I., De Los Santos, E. L. C., Yeong, M., Cruz-Morales, P., Abubucker, S., Roeters, A., Lokhorst, W., Fernandez-Guerra, A., Cappelini, L. T. D., Goering, A. W., Thomson, R. J., Metcalf, W. W., Kelleher, N. L., Barona-Gomez, F., & Medema, M. H. (2019). A computational framework to explore large-scale biosynthetic diversity. *Nature Chemical Biology*, 1–9. https://doi.org/10.1038/s41589-019-0400-9

Oh, Y., Donofrio, N., Pan, H., Coughlan, S., Brown, D. E., Meng, S., Mitchell, T., & Dean, R. A. (2008). Transcriptome analysis reveals new insight into appressorium formation and function in the rice blast fungus Magnaporthe oryzae. *Genome Biology*, *9*(5), R85. https://doi.org/10.1186/gb-2008-9-5-r85

Oliva, R. F., Cano, L. M., Raffaele, S., Win, J., Bozkurt, T. O., Belhaj, K., Oh, S.-K., Thines, M., & Kamoun, S. (2015). A Recent Expansion of the RXLR Effector Gene *Avrblb2* Is Maintained in Global Populations of *Phytophthora infestans* Indicating Different Contributions to Virulence. *Molecular Plant-Microbe Interactions®*, *28*(8), 901–912. https://doi.org/10.1094/MPMI-12-14-0393-R

Palma-Guerrero, J., Ma, X., Torriani, S. F. F., Zala, M., Francisco, C. S., Hartmann, F. E., Croll, D., & McDonald, B. A. (2017). Comparative Transcriptome Analyses in Zymoseptoria tritici Reveal Significant Differences in Gene Expression Among Strains During Plant Infection. *Molecular Plant-Microbe Interactions: MPMI*, *30*(3), 231–244. https://doi.org/10.1094/MPMI-07-16-0146-R

Patkar, R. N., Benke, P. I., Qu, Z., Constance Chen, Y. Y., Yang, F., Swarup, S., & Naqvi, N. I. (2015). A fungal monooxygenase-derived jasmonate attenuates host innate immunity. *Nature Chemical Biology*, *11*(9), 733–740. https://doi.org/10.1038/nchembio.1885

Patkar, R. N., & Naqvi, N. I. (2017). Fungal manipulation of hormone-regulated plant defense. *PLoS Pathogens*, *13*(6), 10–14. https://doi.org/10.1371/journal.ppat.1006334

Patkar, R. N., Ramos-Pamplona, M., Gupta, A. P., Fan, Y., & Naqvi, N. I. (2012). Mitochondrial β-oxidation regulates organellar integrity and is necessary for conidial germination and invasive growth in *Magnaporthe oryzae*: Mitochondrial β-oxidation in *Magnaporthe*. *Molecular Microbiology*, *86*(6), 1345–1363. https://doi.org/10.1111/mmi.12060

Price, M. N., Dehal, P. S., & Arkin, A. P. (2010). FastTree 2 – Approximately Maximum-Likelihood Trees for Large Alignments. *PLoS ONE*, *5*(3), e9490. https://doi.org/10.1371/journal.pone.0009490

Rahnama, M., Novikova, O., Starnes, J. H., Zhang, S., Chen, L., & Farman, M. L. (2020). Transposon-mediated telomere destabilization: A driver of genome evolution in the blast fungus. *Nucleic Acids Research*, gkaa287. https://doi.org/10.1093/nar/gkaa287

Rahnama, M., Wang, B., Dostart, J., Novikova, O., Yackzan, D., Yackzan, A., Bruss, H., Baker, M., Jacob, H., Zhang, X., Lamb, A., Stewart, A., Heist, M., Hoover, J., Calie, P., Chen, L., Liu, J., & Farman, M. L. (2021). Telomere Roles in Fungal Genome Evolution and Adaptation. *Frontiers in Genetics*, *12*, 676751. https://doi.org/10.3389/fgene.2021.676751

Rozas, J., Ferrer-Mata, A., Sánchez-DelBarrio, J. C., Guirao-Rico, S., Librado, P., Ramos-Onsins, S. E., & Sánchez-Gracia, A. (2017). DnaSP 6: DNA Sequence Polymorphism Analysis of Large Data Sets. *Molecular Biology and Evolution*, *34*(12), 3299–3302. https://doi.org/10.1093/molbev/msx248

Rudd, J. J., Kanyuka, K., Hassani-Pak, K., Derbyshire, M., Andongabo, A., Devonshire, J., Lysenko, A., Saqi, M., Desai, N. M., Powers, S. J., Hooper, J., Ambroso, L., Bharti, A., Farmer, A., Hammond-Kosack, K. E., Dietrich, R. A., & Courbot, M. (2015). Transcriptome and metabolite profiling of the infection cycle of Zymoseptoria tritici on wheat reveals a biphasic interaction with plant immunity involving differential pathogen chromosomal contributions and a variation on the hemibiotrophic lifestyle definition. *Plant Physiology*, *167*(3), 1158–1185. https://doi.org/10.1104/pp.114.255927

Sánchez-Vallet, A., Fouché, S., Fudal, I., Hartmann, F. E., Soyer, J. L., Tellier, A., & Croll, D. (2018). The Genome Biology of Effector Gene Evolution in Filamentous Plant Pathogens. *Annual Review of Phytopathology*, *56*(1), 21–40. https://doi.org/10.1146/annurev-phyto-080516-035303

Shannon, P., Markiel, A., Ozier, O., Baliga, N. S., Wang, J. T., Ramage, D., Amin, N., Schwikowski, B., & Ideker, T. (2003). Cytoscape: A Software Environment for Integrated Models of Biomolecular Interaction Networks. *Genome Research*, *13*(11), 2498–2504. https://doi.org/10.1101/GR.1239303

Shen, Q., Liu, Y., & Naqvi, N. I. (2018). Fungal effectors at the crossroads of phytohormone signaling. *Current Opinion in Microbiology*, *46*, 1–6. https://doi.org/10.1016/J.MIB.2018.01.006

Simão, F. A., Waterhouse, R. M., Ioannidis, P., Kriventseva, E. V., & Zdobnov, E. M. (2015). BUSCO: assessing genome assembly and annotation completeness with single-copy orthologs. *Bioinformatics*, *31*(19), 3210–3212. https://doi.org/10.1093/BIOINFORMATICS/BTV351

Soundararajan, S., Jedd, G., Li, X., Ramos-pamplon, M., Chua, N. H., & Naqvi, N. I. (2004). Woronin body function in Magnaporthe grisea is essential for efficient pathogenesis and for survival during nitrogen starvation stress. *The Plant Cell*, *16*(June), 1564–1574. https://doi.org/10.1105/tpc.020677.2001

Stanke, M., Schöffmann, O., Morgenstern, B., & Waack, S. (2006). Gene prediction in eukaryotes with a generalized hidden Markov model that uses hints from external sources. *BMC Bioinformatics*, *7*(1), 1–11. https://doi.org/10.1186/1471-2105-7-62/TABLES/2

Starnes, J. H., Thornbury, D. W., Novikova, O. S., Rehmeyer, C. J., & Farman, M. L. (2012). Telomere-Targeted Retrotransposons in the Rice Blast Fungus *Magnaporthe oryzae:* Agents of Telomere Instability. *Genetics*, *191*(2), 389–406. https://doi.org/10.1534/genetics.111.137950

Talbot, N. J. (2003). On the Trail of a Cereal Killer: Exploring the Biology of Magnaporthe grisea. *Annual Review of Microbiology*, *57*(1), 177–202. https://doi.org/10.1146/annurev.micro.57.030502.090957

Tsuge, T., Harimoto, Y., Akimitsu, K., Ohtani, K., Kodama, M., Akagi, Y., Egusa, M., Yamamoto, M., & Otani, H. (2013). Host-selective toxins produced by the plant pathogenic fungus *Alternaria alternata*. *FEMS Microbiology Reviews*, *37*(1), 44–66. https://doi.org/10.1111/j.1574-6976.2012.00350.x

Van Der Hoorn, R. (2002). Balancing selection favors guarding resistance proteins. *Trends in Plant Science*, *7*(2), 67–71. https://doi.org/10.1016/S1360-1385(01)02188-4

Vy, T. T. P., Inoue, Y., Asuke, S., Chuma, I., Nakayashiki, H., & Tosa, Y. (2024). The ACE1 secondary metabolite gene cluster is a pathogenicity factor of wheat blast fungus. *Communications Biology*, *7*(1), 812. https://doi.org/10.1038/s42003-024-06517-7

Walton, J. D. (2006). HC-toxin. *Phytochemistry*, *67*(14), 1406–1413. https://doi.org/10.1016/j.phytochem.2006.05.033

Yan, X., Tang, B., Ryder, L. S., MacLean, D., Were, V. M., Eseola, A. B., Cruz-Mireles, N., Ma, W., Foster, A. J., Osés-Ruiz, M., & Talbot, N. J. (2023). The transcriptional landscape of plant infection by the rice blast fungus *Magnaporthe oryzae* reveals distinct families of temporally co-regulated and structurally conserved effectors. *The Plant Cell*, koad036. https://doi.org/10.1093/plcell/koad036

Yoshida, K., Saunders, D. G. O., Mitsuoka, C., Natsume, S., Kosugi, S., Saitoh, H., Inoue, Y., Chuma, I., Tosa, Y., Cano, L. M., Kamoun, S., & Terauchi, R. (2016). Host

specialization of the blast fungus Magnaporthe oryzae is associated with dynamic gain and loss of genes linked to transposable elements. *BMC Genomics*, *17*(1), 370. https://doi.org/10.1186/s12864-016-2690-6

Zhong, Z., Norvienyeku, J., Chen, M., Bao, J., Lin, L., Chen, L., Lin, Y., Wu, X., Cai, Z., Zhang, Q., Lin, X., Hong, Y., Huang, J., Xu, L., Zhang, H., Chen, L., Tang, W., Zheng, H., Chen, X., … Nielsen, R. (2016). Directional Selection from Host Plants Is a Major Force Driving Host Specificity in Magnaporthe Species. *Scientific Reports*, *6*, 25591. https://doi.org/10.1038/srep25591

853 **Figure captions**

854

855 **Figure 1. *Pyricularia oryzae* worldwide populations are organized in host-specific**
856 **lineages.** A) Geographic distribution of sequenced *P. oryzae* strains. The color-coded dots
857 denote the host plant of origin of the strains. B) Phylogenetic tree constructed based on
858 concatenation of 2655 BUSCO genes present in all 68 *P. oryzae* genomes used in this study.
859 Colored shapes in the background depict different host-specific genetic lineages.

860

861 **Figure 2. Similarity network analysis of biosynthetic gene clusters (BGCs) from**
862 ***Pyricularia oryzae* and *Pyricularia grisea*.** A BiG-SCAPE analysis with a cutoff c0.5 depicts
863 similarity of 4224 BGCs from *P. oryzae* or *P. grisea* with 277 reference BGCs from MIBiG
864 database. Each dot represents a BGC and is color-coded according to the lineage. Gene cluster
865 families (GCF; subnetworks) marked with green boxes share significant homology with
866 reference MIBiG BGCs (grey-colored circle). GCFs marked with red boxes are found to be
867 unique to host-specific lineages. The length of the gray lines is proportional to the genetic
868 distance between BGCs. Singletons are shown as individual dots at the bottom.

869

870 **Figure 3. BGC-O1 is predominantly present in *Oryza* lineage of *Pyricularia oryzae*.** BiG-
871 SCAPE network showing BGC-O1 present in 23 genomes from *Oryza* and one genome from
872 *Eragrostis* lineages. Conservation of the BGC in selected strains is depicted using Clinker.
873 Vertical bars besides the name of strain are colored according to the lineages. Red and gray
874 dashed boxes separate BGC-O1 and BGC-O1-like clusters, respectively.

875

876 **Figure 4. Genomic localization of BGC-O1 and synteny between the *Oryza* and non-**
877 ***Oryza* lineages.** A) Synteny analysis using pairwise comparison within *Oryza* lineage.
878 Genomes of GUY11 and FR13 aligned individually with reference genome 70-15. The
879 syntenic BGC-O1 locus (orange) and the flanking regions (blue) on chromosome 2 of 70-15
880 are depicted. The differential lengths of BGC-O1 in different isolates are marked with a bar
881 and corresponding length in kilobases. The black arrowhead depicts genomic rearrangement
882 (swapping) in the flanking ~10 Kb region. The red arrowhead marks the rearrangement of ~9
883 Kb region of the BGC-O1 in FR13. B) Synteny analyses of representative genome assemblies
884 belonging to *Setaria* (US71), *Eleusine* (MZ5-1-6 and CD156) and *Oryza* (70-15) lineages.
885 The BGC-O1 locus (orange) and flanking region (blue) sequences from US71, MZ5-1-6 and
886 CD156 aligned with that of 70-15 are depicted.

887

888 **Figure 5. Evolutionary origin of the reducing polyketide synthase (PKS) MGG_08236**
889 **gene.** A) Maximum-likelihood phylogenetic tree using protein sequences of reducing PKS
890 genes from BGC-O1 and related gene cluster families, as well as homologues retrieved from
891 MycoCosm repository. Tip labels depicting sequences from *Oryza* and *Eragrostis*-specific
892 clade are marked with blue and pink background, respectively. The *Colletotrichum*
893 *eremocloae* ortholog (jgi.p_Coler1_670826), closer to MGG_08236, is denoted with pink
894 label; whereas the more distant paralogue (jgi.p_Coler1_679399) is shown in orange. Gray
895 shaded triangles denote collapsed clades with distant sequences. Branches were supported by
896 > 95% Bootstrap values indicated with gray circles at the nodes. The tree is rooted at

897 midpoint. B) Comparative analysis, using Clinker tool, of the BGC-O1 or BGC-O1-like loci
898 from three *Oryza*-specific and *C. eremochloae* genomes.

899

900 **Figure 6. BGC-O1 genes are specifically expressed during pathogenic development.** A)
901 Gel electrophoresis of PCR products displaying presence or absence of ORF region of rPKS
902 MGG_08236 from genomic DNA of the indicated *P. oryzae* strains. B157, MOS2, MOS3 and
903 MOS5 belong to the *Oryza* lineage (labelled in blue); whereas, the MOS1, MEC1, MEC4,
904 MEC5, MEC6 and MEA1 belong to the *Eleusine* lineage (labelled in red). * - the only *Oryza*
905 strain that lacked the BGC-O1 in *in-silico* analysis. ** - the *Oryza* strains placed outside
906 *Oryza* lineage. Arrowheads corresponds to the 1 Kb size of band from Marker. B) RT-PCR
907 gel depicting expression of genes MGG_08236 (Polyketide synthase), MGG_15107 (Methyl
908 transferase), MGG_15108 (Co-A transferase) and MGG_12496 (Cytochrome P450) in *Oryza*-
909 specific strain B157 at different stages of rice infection (12 to 96 hours post inoculation) and
910 during vegetative growth (mycelium) in complete medium.

911

912 **Supplementary Information**
913
914
915 **Supplementary tables:**
916
917 **Supplementary Table S1:** *Pyricularia oryzae* and *Pyricularia grisea* genomes used in this
918 study.
919 **Supplementary Table S2:** *De novo* assembly statistics and gene prediction content of
920 *Pyricularia oryzae* strains sequenced in this study.
921 **Supplementary Table S3:** Number of BGCs predicted using fungiSMASH in this study.
922 **Supplementary Table S4:** Summary of population genetic variation in 40 core biosynthetic
923 genes in *Oryza*, *Eleusine* and *Triticum* lineages of *P. oryzae*.
924 **Supplementary Table S5:** Oligonucleotide primers used to study the relative expression of
925 BGC-O1 genes.
926
927
928 **Supplementary figures:**
929
930 **Supplementary Figure S1:** *Pyricularia oryzae* and *Pyricularia grisea* are evolutionarily
931 distinct species adapted to different hosts.
932 **Supplementary Figure S2:** Pathogenicity tests of *P. oryzae* strains isolated from different
933 hosts and geographic locations in India.
934 **Supplementary Figure S3:** Occurrence of BGCs associated with specific classes of SM in
935 individual genomes of *P. oryzae* and *P. grisea*.
936 **Supplementary Figure S4:** Homology of melanin-associated *P. oryzae* and *P. grisea* gene
937 cluster family with reference BGCs in MIBiG database.
938 **Supplementary Figure S5:** Analysis of homology between *ACE1* gene cluster family in *P.*
939 *oryzae* and *P. grisea* and reference BGCs in MIBiG database.
940 **Supplementary Figure S6:** Analysis of homology between putative epipyriculol-associated
941 gene cluster family in *P. oryzae* and *P. grisea* and reference BGCs in MIBiG database.
942 **Supplementary Figure S7:** Homology of putative Squalestatin S1-associated *P. oryzae* and
943 *P. grisea* gene cluster family with reference BGCs in MIBiG database.
944 **Supplementary Figure S8:** Analysis of homology between Tenuazonic acid-associated gene
945 cluster families in host-adapted *P. oryzae* and *P. grisea* isolates.
946 **Supplementary Figure S9:** BGC-O2 is predominantly present in *Oryza*-specific lineage of *P.*
947 *oryzae*.
948 **Supplementary Figure S10:** BGC-TLE is predominantly present in *Triticum*, *Lolium* and
949 *Eleusine*-specific lineages of *P. oryzae*.
950 **Supplementary Figure S11:** Comparison of core biosynthetic gene region of BGC-TLE
951 shows the pseudogenization in NRPS gene belonging to *Triticum* lineage.
952
953 **Supplementary datasets:**
954
955 **Supplementary dataset S1:** Amino acid sequences of 2655 BUSCOs present in 68 strains of
956 *P. oryzae*.
957 **Supplementary dataset S2:** Amino acid sequence alignments of 2655 BUSCOs present in 68
958 strains of *P. oryzae*.

959 **Supplementary dataset S3:** Best partitioning scheme used to construct Maximum-likelihood
960 tree for *P. oryzae* strains.
961 **Supplementary dataset S4:** Maximum-likelihood tree based on 2655 BUSCOs present in 68
962 strains of *P. oryzae*.
963 **Supplementary dataset S5:** Amino acid sequences of 2557 BUSCOs present in 71 strains of
964 *P. oryzae* and *P. grisea*.
965 **Supplementary dataset S6:** Amino acid sequence alignments of 2557 BUSCOs present in 71
966 strains of *P. oryzae* and *P. grisea*.
967 **Supplementary dataset S7:** Maximum-likelihood tree based on 2557 BUSCOs present in 71
968 strains of *P. oryzae* and *P. grisea*.
969 **Supplementary dataset S8:** Manually curated gene models from *Oryza*-lineage-specific
970 BGC-O1.
971 **Supplementary dataset S9:** Amino acid sequences of the subset of rPKS (MGG_08236)
972 homologs in *Pezizomycotina* group.
973 **Supplementary dataset S10:** Amino acid sequence alignments of the subset of rPKS
974 (MGG_08236) homologs in *Pezizomycotina* group.
975 **Supplementary dataset S11:** Maximum-likelihood tree based on the subset of rPKS
976 (MGG_08236) homologs in *Pezizomycotina* group.

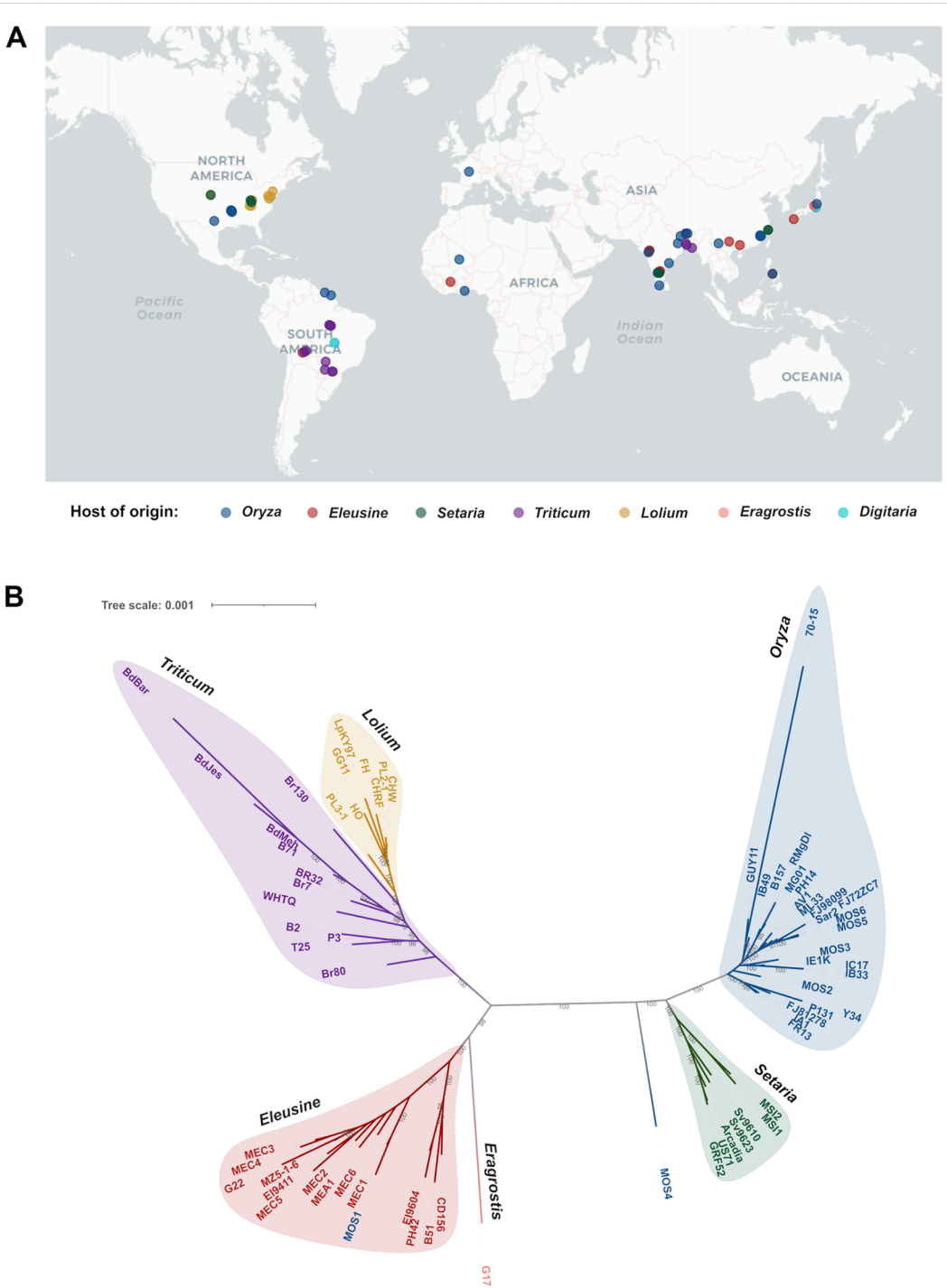
A
NORTH AMERICA
ASIA
AFRICA
Pacific Ocean
SOUTH AMERICA
Indian Ocean
OCEANIA
Host of origin:
Oryza
Eleusine
Setaria
Triticum
Lolium
Eragrostis
Digitaria
B
Tree scale: 0.001
Triticum
BdBar
BdJes
Br130
BdMeh
Br71
BR32
Br7
WHTQ
B2
P3
T25
Br80
Lolium
LpKY97
GG11
FH
PL2-1
CHW
CHRF
PL3-1
HO
Oryza
70-15
GUY11
IB49
B157
RMgDI
MG01
PH14
AV1-1
MLT33
FJ98099
Sar2
FJ72ZC7
MOS6
MOS5
MOS3
IE1K
IC17
IB33
MOS2
P131
Y34
FJB1278
IA7
FR13
Setaria
MSI2
MSI1
Sv9610
Sv9623
Arcadia
US71
GRF52
MOS4
Eleusine
MEC3
MEC4
G22
MZ5-1-6
EI9411
MEC5
MEC2
MEA1
MEC6
MEC1
MOS1
EI9604
PH42
B51
CD156
Eragrostis
G17

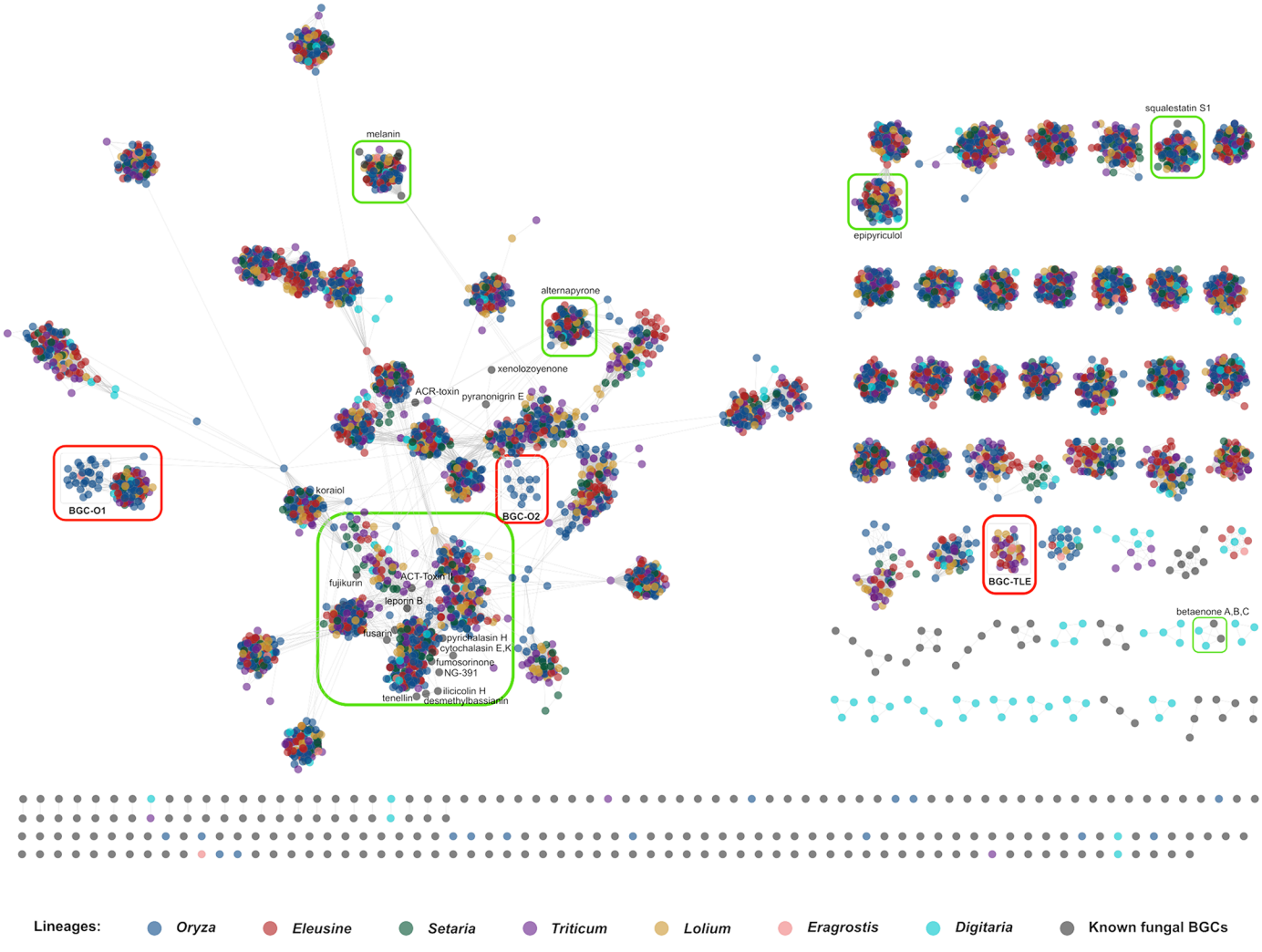
melanin
alternapyrone
xenolozoyenone
ACR-toxin
pyranonigrin E
BGC-O1
koraiol
BGC-O2
ACT-Toxin II
fujikurin
leporin B
fusarin
pyrichalasin H
cytochalasin E,K
fumosorinone
NG-391
tenellin
desmethylbassianin
ilicicolin H
squalestatin S1
epipyriculol
BGC-TLE
betaenone A,B,C
Lineages:
Oryza
Eleusine
Setaria
Triticum
Lolium
Eragrostis
Digitaria
Known fungal BGCs

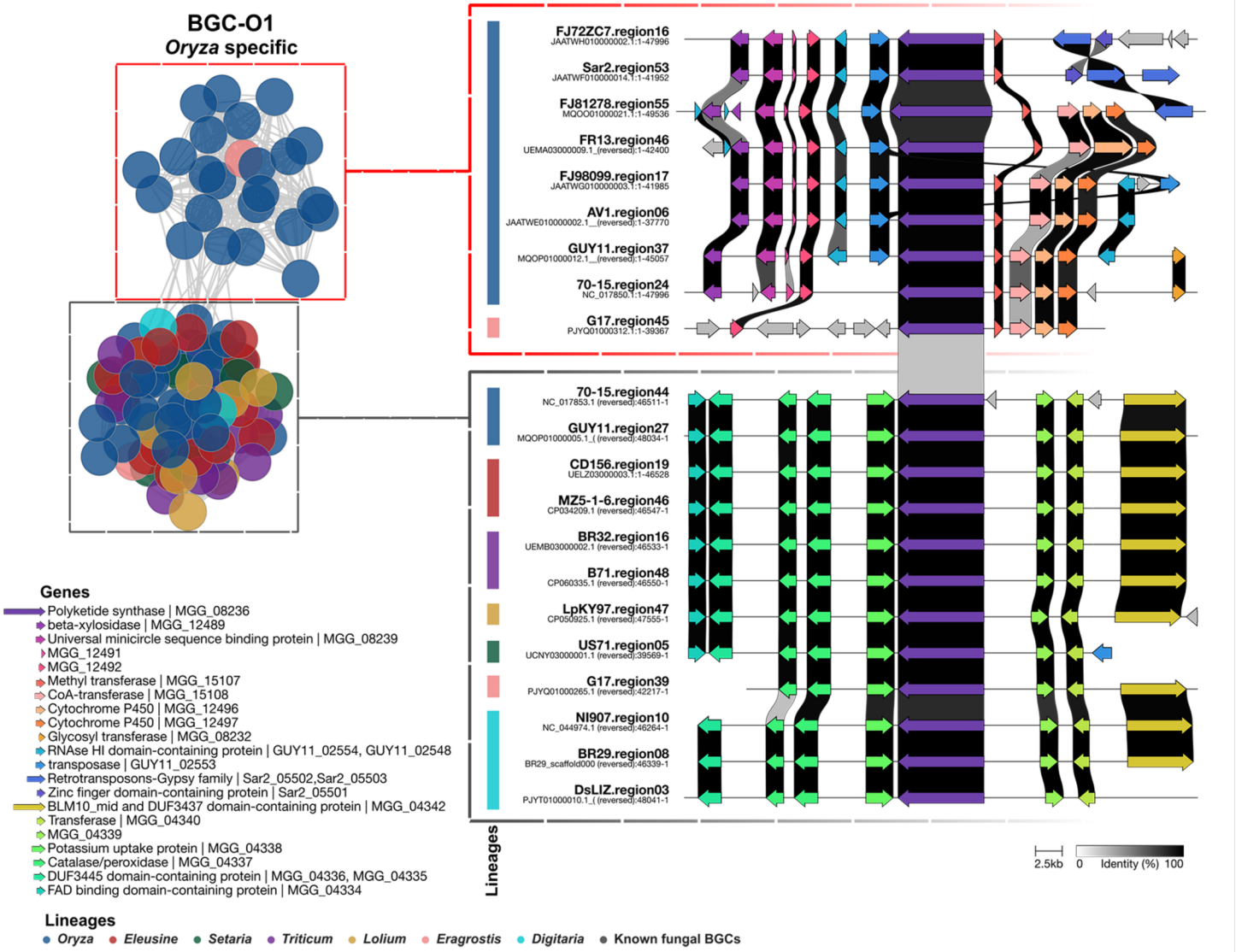
BGC-O1
Oryza specific
FJ72ZC7.region16
JAATWH010000002.1:1-47996
Sar2.region53
JAATWF010000014.1:1-41952
FJ81278.region55
MQOO01000021.1:1-49536
FR13.region46
UEMA03000009.1_(reversed):1-42400
FJ98099.region17
JAATWG010000003.1:1-41985
AV1.region06
JAATWE010000002.1_(reversed):1-37770
GUY11.region37
MQOP01000012.1_(reversed):1-45057
70-15.region24
NC_017850.1:1-47996
G17.region45
PJYQ01000312.1:1-39367
70-15.region44
NC_017853.1 (reversed):46511-1
GUY11.region27
MQOP01000005.1_((reversed):48034-1
CD156.region19
UELZ03000003.1:1-46528
MZ5-1-6.region46
CP034209.1 (reversed):46547-1
BR32.region16
UEMB03000002.1 (reversed):46533-1
B71.region48
CP060335.1 (reversed):46550-1
LpKY97.region47
CP050925.1 (reversed):47555-1
US71.region05
UCNY03000001.1 (reversed):39569-1
G17.region39
PJYQ01000265.1 (reversed):42217-1
NI907.region10
NC_044974.1 (reversed):46264-1
BR29.region08
BR29_scaffold000 (reversed):46339-1
DsLIZ.region03
PJYT01000010.1_((reversed):48041-1
Lineages
2.5kb
0
Identity (%) 100
Genes
Polyketide synthase | MGG_08236
beta-xylosidase | MGG_12489
Universal minicircle sequence binding protein | MGG_08239
MGG_12491
MGG_12492
Methyl transferase | MGG_15107
CoA-transferase | MGG_15108
Cytochrome P450 | MGG_12496
Cytochrome P450 | MGG_12497
Glycosyl transferase | MGG_08232
RNAse HI domain-containing protein | GUY11_02554, GUY11_02548
transposase | GUY11_02553
Retrotransposons-Gypsy family | Sar2_05502,Sar2_05503
Zinc finger domain-containing protein | Sar2_05501
BLM10_mid and DUF3437 domain-containing protein | MGG_04342
Transferase | MGG_04340
MGG_04339
Potassium uptake protein | MGG_04338
Catalase/peroxidase | MGG_04337
DUF3445 domain-containing protein | MGG_04336, MGG_04335
FAD binding domain-containing protein | MGG_04334
Lineages
Oryza
Eleusine
Setaria
Triticum
Lolium
Eragrostis
Digitaria
Known fungal BGCs

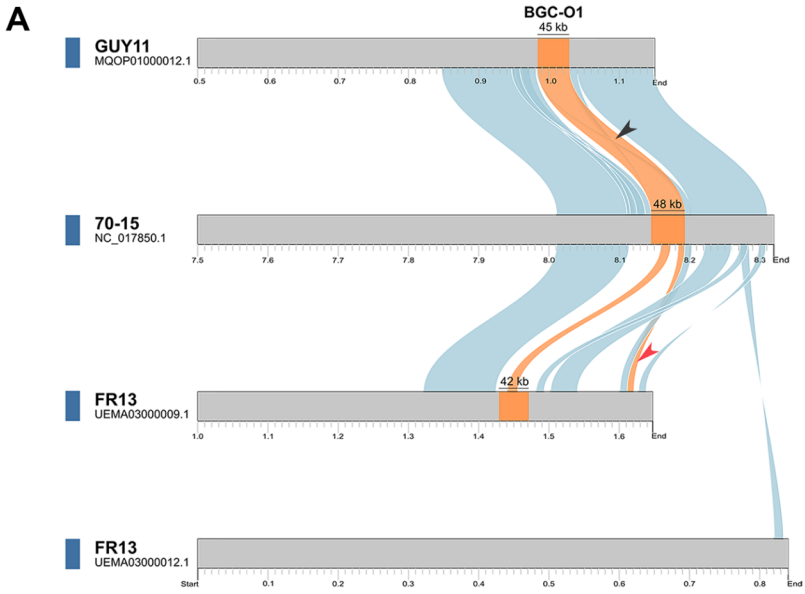
A
BGC-O1
45 kb
GUY11
MQOP01000012.1
0.5
0.6
0.7
0.8
0.9
1.0
1.1
End
48 kb
70-15
NC_017850.1
7.5
7.6
7.7
7.8
7.9
8.0
8.1
8.2
8.3
End
42 kb
FR13
UEMA03000009.1
1.0
1.1
1.2
1.3
1.4
1.5
1.6
End
FR13
UEMA03000012.1
Start
0.1
0.2
0.3
0.4
0.5
0.6
0.7
0.8
End

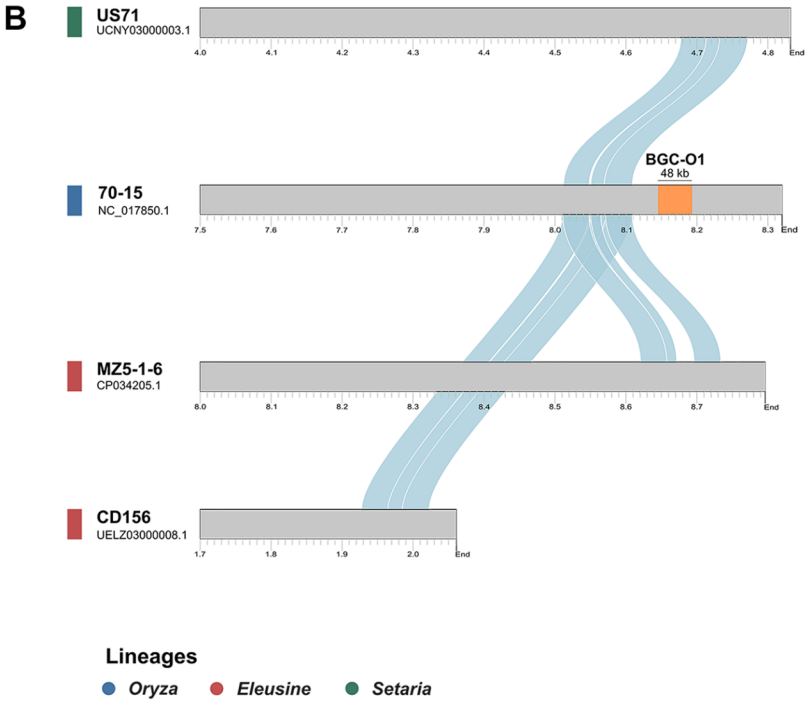
B
US71
UCNY03000003.1
4.0
4.1
4.2
4.3
4.4
4.5
4.6
4.7
4.8
End
BGC-O1
48 kb
70-15
NC_017850.1
7.5
7.6
7.7
7.8
7.9
8.0
8.1
8.2
8.3
End
MZ5-1-6
CP034205.1
8.0
8.1
8.2
8.3
8.4
8.5
8.6
8.7
End
CD156
UELZ03000008.1
1.7
1.8
1.9
2.0
End
Lineages
Oryza
Eleusine
Setaria

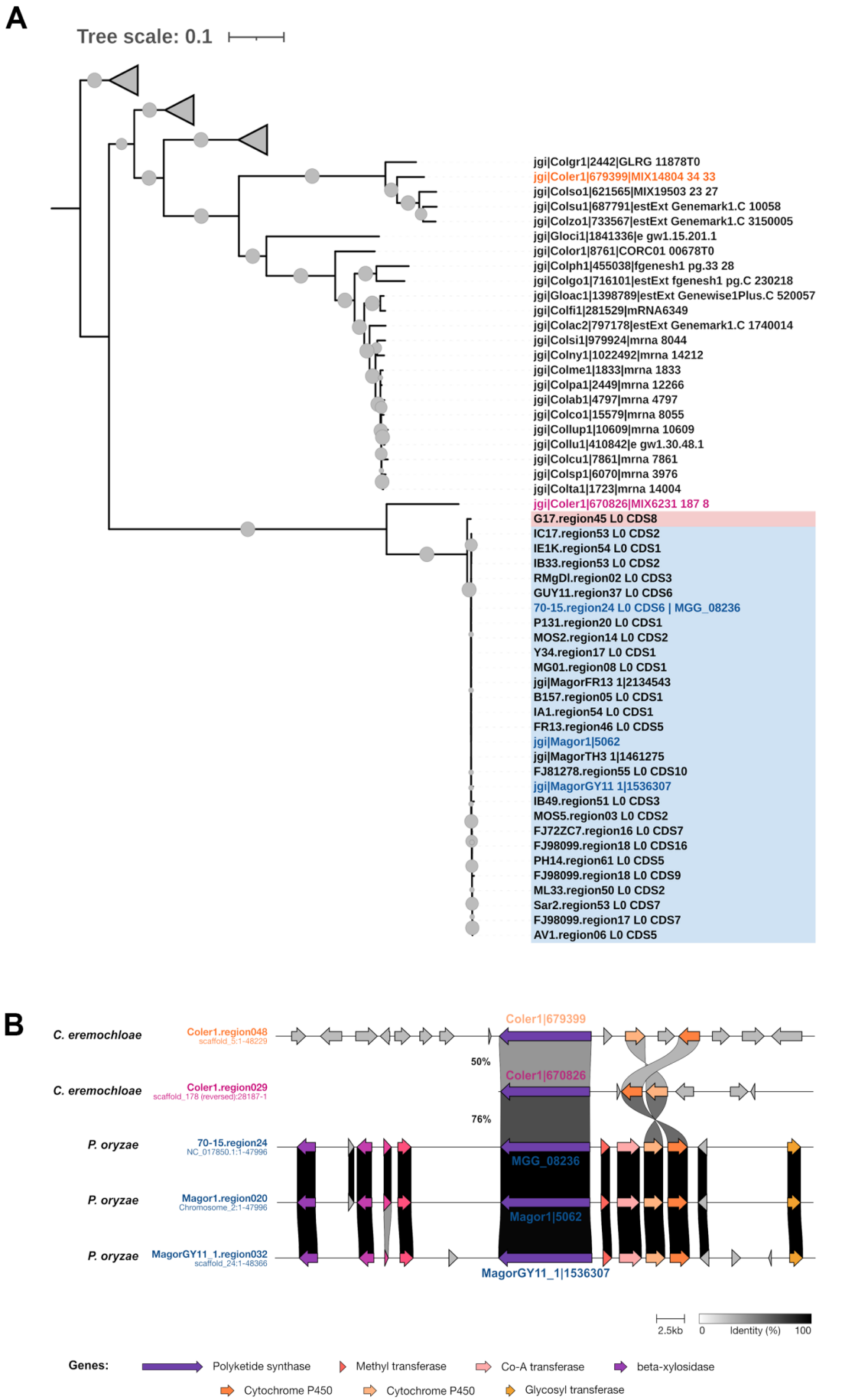
A
Tree scale: 0.1
jgi|Colgr1|2442|GLRG 11878T0
jgi|Coler1|679399|MIX14804 34 33
jgi|Colso1|621565|MIX19503 23 27
jgi|Colsu1|687791|estExt Genemark1.C 10058
jgi|Colzo1|733567|estExt Genemark1.C 3150005
jgi|Gloci1|1841336|e gw1.15.201.1
jgi|Color1|8761|CORC01 00678T0
jgi|Colph1|455038|fgenesh1 pg.33 28
jgi|Colgo1|716101|estExt fgenesh1 pg.C 230218
jgi|Gloac1|1398789|estExt Genewise1Plus.C 520057
jgi|Colfi1|281529|mRNA6349
jgi|Colac2|797178|estExt Genemark1.C 1740014
jgi|Colsi1|979924|mrna 8044
jgi|Colny1|1022492|mrna 14212
jgi|Colme1|1833|mrna 1833
jgi|Colpa1|2449|mrna 12266
jgi|Colab1|4797|mrna 4797
jgi|Colco1|15579|mrna 8055
jgi|Collup1|10609|mrna 10609
jgi|Collu1|410842|e gw1.30.48.1
jgi|Colcu1|7861|mrna 7861
jgi|Colsp1|6070|mrna 3976
jgi|Colta1|1723|mrna 14004
jgi|Coler1|670826|MIX6231 187 8
G17.region45 L0 CDS8
IC17.region53 L0 CDS2
IE1K.region54 L0 CDS1
IB33.region53 L0 CDS2
RMgDl.region02 L0 CDS3
GUY11.region37 L0 CDS6
70-15.region24 L0 CDS6 | MGG_08236
P131.region20 L0 CDS1
MOS2.region14 L0 CDS2
Y34.region17 L0 CDS1
MG01.region08 L0 CDS1
jgi|MagorFR13 1|2134543
B157.region05 L0 CDS1
IA1.region54 L0 CDS1
FR13.region46 L0 CDS5
jgi|Magor1|5062
jgi|MagorTH3 1|1461275
FJ81278.region55 L0 CDS10
jgi|MagorGY11 1|1536307
IB49.region51 L0 CDS3
MOS5.region03 L0 CDS2
FJ72ZC7.region16 L0 CDS7
FJ98099.region18 L0 CDS16
PH14.region61 L0 CDS5
FJ98099.region18 L0 CDS9
ML33.region50 L0 CDS2
Sar2.region53 L0 CDS7
FJ98099.region17 L0 CDS7
AV1.region06 L0 CDS5
B
C. eremochloae
Coler1.region048
scaffold_5:1-48229
Coler1|679399
50%
C. eremochloae
Coler1.region029
scaffold_178 (reversed):28187-1
Coler1|670826
76%
P. oryzae
70-15.region24
NC_017850.1:1-47996
MGG_08236
P. oryzae
Magor1.region020
Chromosome_2:1-47996
Magor1|5062
P. oryzae
MagorGY11_1.region032
scaffold_24:1-48366
MagorGY11_1|1536307
2.5kb
0
Identity (%)
100
Genes:
Polyketide synthase
Methyl transferase
Co-A transferase
beta-xylosidase
Cytochrome P450
Cytochrome P450
Glycosyl transferase

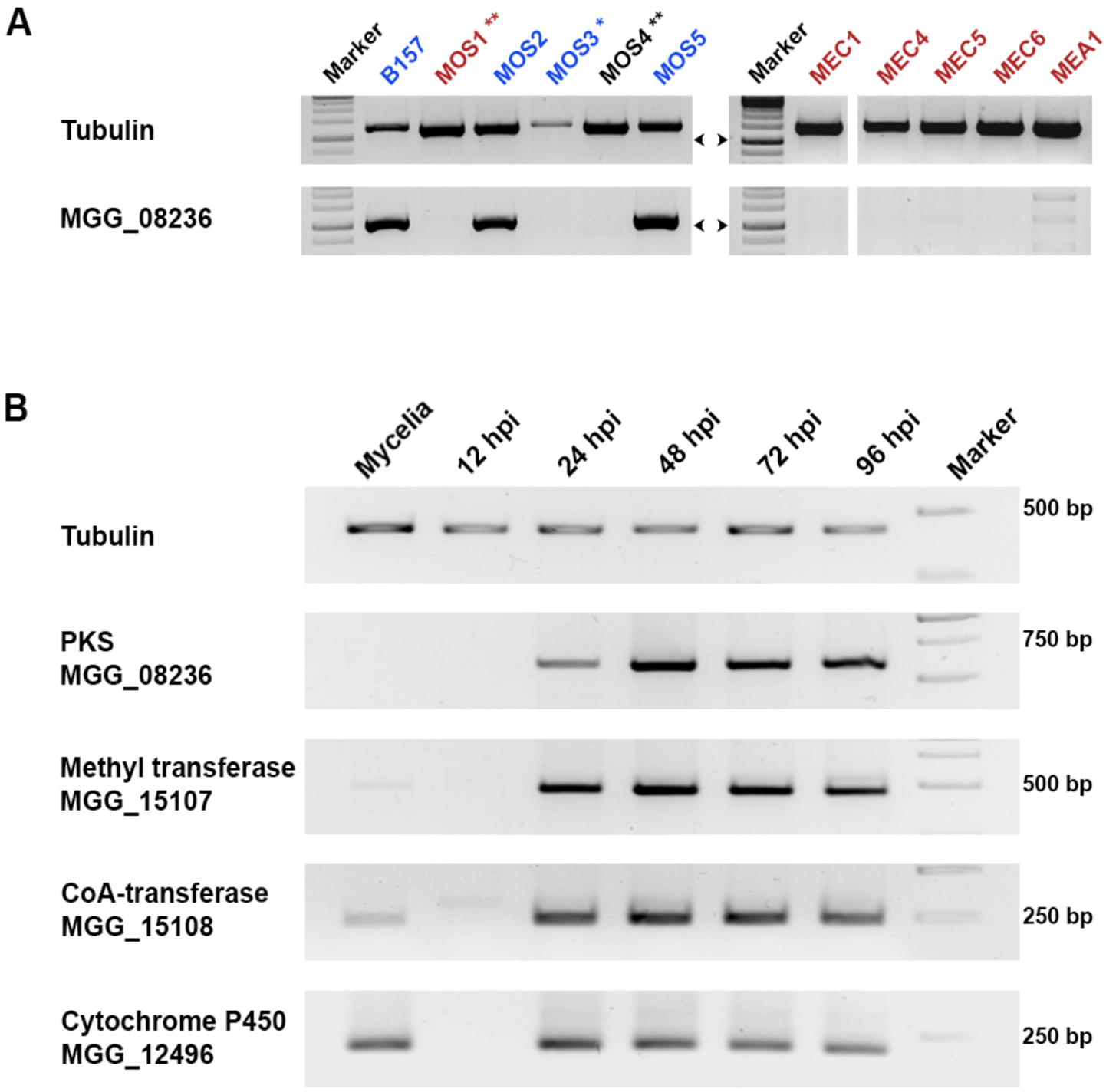
A
Marker
B157
MOS1 **
MOS2
MOS3 *
MOS4 **
MOS5
Marker
MEC1
MEC4
MEC5
MEC6
MEA1
Tubulin
MGG_08236
B
Mycelia
12 hpi
24 hpi
48 hpi
72 hpi
96 hpi
Marker
Tubulin
500 bp
PKS
MGG_08236
750 bp
Methyl transferase
MGG_15107
500 bp
CoA-transferase
MGG_15108
250 bp
Cytochrome P450
MGG_12496
250 bp